CONTROLLING LUMINESCENT AND THERMORESPONSIVE MATERIALS WITH MOLECULAR PHOTOSWITCHING

by

Zach Erno
B.Sc., Arizona State University, 2006

THESIS SUBMITTED IN PARTIAL FULFILLMENT OF
THE REQUIREMENTS FOR THE DEGREE OF

MASTER OF SCIENCE

In the
Department of Chemistry
Faculty of Science

SIMON FRASER UNIVERSITY

Summer 2012

APPROVAL

Name: **Zach Erno**

Degree: **Master of Science**

Title of Thesis: **Controlling Luminescent and Thermoresponsive Materials with Molecular Photoswitching**

Examining Committee:

Chair **Dr. Hua-Zhong Yu**
Professor, Department of Chemistry

Dr. Neil Branda
Senior Supervisor
Professor, Department of Chemistry

Dr. Charles Walsby
Supervisor
Associate Professor, Department of Chemistry

Dr. Vance Williams
Supervisor
Associate Professor, Department of Chemistry

Dr. Peter Wilson
Internal Examiner
Associate Professor, Department of Chemistry

Date Defended: July 30, 2012

Partial Copyright Licence

ABSTRACT

Molecular switching motifs based on dithienylethenes provide a versatile framework for developing materials whose properties can be toggled between two states by alternately exposing them to ultraviolet and visible light. Materials with these features can then be selectively addressed and their properties manipulated even when present in complex mixtures, making them attractive for applications in controlled drug delivery, catalysis and imaging. Developing these materials nevertheless requires design strategies that couple light-induced changes in the dithienylethene architecture to desirable secondary events (*e.g.* changes in catalytic or biological activity, refractive index, or electrical resistance). This thesis describes analogous design strategies developed to control luminescent and thermoresponsive materials using optical cues. In the first system, quantum dot luminescence is reversibly quenched by photoisomerization of a cationic dithienylethene ligand. In the second, photoisomerization of a bicyclic dithienylfuran adduct is shown to gate the reversibility of the Diels-Alder reaction at elevated temperatures.

Keywords: photochromism, dithienylethene, dithienylfuran, Diels-Alder reaction, quantum dots, self-healing polymers, stimulated emission depletion, Förster resonance energy transfer, electron transfer, luminescence quenching

ACKNOWLEDGEMENTS

I extend my thanks to Dr. Brian Gorodetsky and Dr. Vincent Lemieux for their help with the initial design of the quantum dot and retro-Diels-Alder projects, respectively. I also thank Amir Mahmoud Asadirad for his assistance with the retro-Diels-Alder project and with our initial efforts in the self-healing polymer project. I also extend my thanks to my senior supervisor, Dr. Neil Branda, my committee members, Dr. Charles Walsby and Dr. Vance Williams, and other members of the Branda group, past and present, for challenging me and for providing valuable insight into my various projects.

TABLE OF CONTENTS

LIST OF FIGURES

LIST OF SCHEMES

LIST OF EQUATIONS

LIST OF TABLES

LIST OF ABBREVIATIONS

>	greater than
<	less than
°C	degree Celsius
Å	angstrom
α	cross-section for two-photon absorption
ε_A	acceptor molar extinction coefficient
$\Delta E_{0,0}$	energy of donor luminescence
ΔE_L	lumophore HOMO-LUMO energy gap
ΔE_Q	quencher HOMO-LUMO energy gap
$\Delta G^{\ddagger}_{ET}$	Gibb's energy of activation of photoinduced electron transfer
ΔG°_{ET}	standard Gibb's energy of photoinduced electron transfer
Δλ	width of an absorption or emission band at half-maximum
ε_0	vacuum permittivity
δ	chemical shift
κ	dipole orientation factor
λ	wavelength (in the context of electromagnetic radiation) or reorganizational energy (in the context of Marcus Theory)
λ_{ex}	excitation wavelength
τ_F	fluorescence lifetime

µA	microampere
µL	microliter
µM	micromolar
µm	micrometer
µmol	micromole
Φ_F	quantum yield of fluorescence
a	centre-to-centre separation between electron donor and acceptor
Ac	acyl
Bu	butyl
cm	centimeter
Cy	cyanine dye
d	doublet, in NMR spectroscopy
DA	Diels-Alder
DMF	dimethylformamide
DMSO-d_6	perdeuterated dimethylsulfoxide
DNA	deoxyribonucleic acid
ds	double-stranded
DSC	differential scanning calorimetry
e	elementary charge
E	*E* isomer (in the context of structural isomerism) or efficiency (in the context of Förster resonance energy transfer)
e_r	dielectric constant
E°(A / A•-)	standard reduction potential of an electron transfer acceptor

$E°(D^{\bullet+} / D)$	standard reduction potential of a radical cation, electron transfer donor
ESI	electrospray ionization
Et	ethyl
F	fluorescence intensity
Fc	ferrocene
FMO	frontier molecular orbital
FRET	Förster resonance energy transfer
g	gram
GC/MS	gas chromatography-mass spectrometer
GM	Goeppert-Mayer (unit for expressing two-photon absorption cross sections)
H	hydrogen nuclei, in proton NMR spectroscopy
h	hour
HOMO	highest occupied molecular orbital
HRMS	high-resolution mass spectrometry
Hz	hertz
IR	infrared
irr	irreversible
J	spectral overlap integral, in FRET
J	coupling constant, in NMR spectroscopy
LUMO	lowest unoccupied molecular orbital
M	molar
M	molar mass of a compound, in mass spectrometry

M.p.	melting point
m/z	mass-to-charge ratio
MBP	maltose-binding protein
Me	methyl
MHz	megahertz
min	minute
mL	milliliter
mM	millimolar
mm	millimeter
mV	millivolt
mW	milliwatt
n	refractive index
N_A	Avogadro's number
nA	nanoampere
NCS	*N*-chlorosuccinimide
nm	nanometer
NMR	nuclear magnetic resonance
ns	nanosecond
p	pentet, in NMR spectroscopy
PEG	poly(ethylene)glycol
Ph	phenyl
pK_a	negative logarithm of an acid dissociation constant

PSS_{λ}	photostationary state at wavelength λ
Q_0	quantum yield of donor luminescence in the absence of a quencher, in FRET
QD	quantum dot
r	centre-to-centre distance between two designated structures
R_0	Förster radius, in FRET
R_n	generalized chemical substituent; may be designated by a numerical subscript “n” (*i.e.* $n \neq 0$)
ROMP	ring-opening metathesis polymerization
s	second
S	singlet, in NMR spectroscopy
S_0	singlet ground state
S_1	first excited singlet state
S_2	second excited singlet state
SCE	saturated calomel electrode
SEM	scanning electron microscopy
sp^2	sp^2 orbital hybrid or hybridization
sp^3	sp^3 orbital hybrid or hybridization
ss	single-stranded
STED	stimulated emission depletion
t	triplet, in NMR spectroscopy
T_n	temperature; may be designated by a numerical subscript “n”
THF	tetrahydrofuran
TMS	tetramethylsilane

TOPO	trioctylphosphine oxide
UV	ultraviolet
vis	visible
V	volt
Z	*Z* isomer

CHAPTER 1: MOLECULAR PHOTOSWITCHING

1.1 Controlling Materials with Light

The ability to selectively manipulate individual materials or compounds within a mixture is potentially beneficial to a wide range of technologies. In industrial polymer manufacture, for instance, the ability to modulate catalyst activity in real-time can help prevent the occurrence of disastrous runaway reactions.[1] Similarly, the pharmaceutical industry depends on the development of compounds capable of targeting pathogens without adversely affecting healthy tissue.[2]

Table 1.1 Relative degrees of control afforded by representative stimuli.

	thermal stimuli	electrical stimuli	optical stimuli
spatial control	poor	good	good
temporal control	poor	good	good
chemical control	poor	poor	good

In many cases, selective control of materials is difficult because of limitations inherent in stimuli conventionally used to affect them (Table 1.1). The use of elevated temperatures is a particularly poor choice for eliciting change in specific components of a mixture because their effects on chemical reaction rates and on the physical parameters of materials are indiscriminate. In addition, the rapid diffusion of heat in condensed phases yields poor spatial control, and the heat ca-

pacities of common materials limit the rate at which elevated temperatures can be attained. Electrical stimuli fare better in terms of spatial and temporal control, benefiting from short response times and the intrinsic confinement of electrochemical reactions to electrode surfaces. However, electrical stimuli affect all materials whose reduction potentials are above or below certain thresholds, resulting in poor chemoselectivity.

The use of optical stimuli is superior in many regards, offering short response times and precise spatial control by adjusting beam dimensions and focal point. Additionally, optical stimuli only affect materials whose electronic energy level spacings match the energy of the light, providing excellent chemoselectivity as well. These benefits feature prominently in photodynamic therapy, in which patients are treated with non-toxic agents that generate cytotoxic effects upon exposure to light, usually in the near-IR. Because the compounds used are inactive before being irradiated, the physician is able to control when and where the drugs are allowed to take effect. Moreover, the selection of compounds that absorb in the near-IR is important because few biological materials absorb or scatter light at these wavelengths, affording deeper tissue penetration and a lower risk of damage to healthy tissues.[3]

Controlling materials with optical stimuli is greatly simplified by design motifs that incorporate molecular photoswitches, which are compounds that undergo bidirectional interconversion between two forms when exposed to light of specific wavelengths.[4] This thesis describes how careful design of dithienylethene photoswitches allows the coupling of features distinct to either form with other physi-

cal or chemical events, enabling control over those events by “toggling” the switch using light of different wavelengths.

1.2 **Dithienylethene Photoswitches**

1.2.1 Structural Features and Photoisomerism

The ring-open dithienylethene structure **1.1o** (Scheme 1.1) generally consists of a carbon-carbon double bond bearing two thiophene substituents oriented *Z* to one another. The other two positions on the carbon-carbon double bond are commonly joined together, forming a cyclic structure, in order to prevent *Z*-*E* isomerization. Structural variation is possible in substituents R^1 and R^2, as well as at carbons 4 and 5 on each of the two thiophenes and in the cyclic structure connecting them.

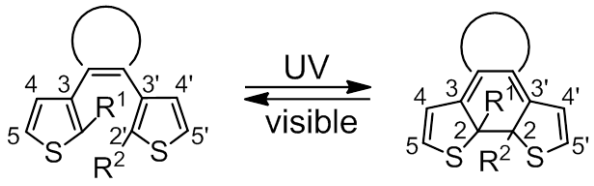

Scheme 1.1 Interconversion of ring-open (**1.1o**) and ring-closed (**1.1c**) dithienylethene isomers using UV and visible light. Structural variation is possible at substituents R^1 and R^2, as well as carbons 4, 4′, 5, and 5′, and in the cyclic structure denoted by an arc.

The ability of each thiophene to rotate independently about the carbon-carbon single bond joining it to the ethene-containing moiety gives rise to two different conformational isomers, which are classified as either *parallel* or *antiparallel* based on whether the substituents R^1 and R^2 are oriented in the same direction or in opposite directions, respectively. Thiophene rotation also limits the de-

gree of pi orbital overlap attainable among the three units and results in an $S_0 \rightarrow S_1$ absorbance positioned in the UV as opposed to longer wavelengths. However, the arrangement of three alternating double bonds, one from the ethene-containing structure and one from each of the two thiophenes, yields sufficient orbital overlap to generate a pi orbital framework reminiscent of *cis*-hexatriene and facilitates an analogous conrotatory electrocyclic reaction that produces isomer **1.1c** upon exposure to UV light.[5]

The electrocyclic reaction that generates **1.1c** joins the two thiophenes to one another by a single bond between carbons 2 and 2′, yielding a six-membered ring (*i.e.* hence the common use of the terms 'ring-open' and 'ring-closed' in reference to photoisomers **1.1o** and **1.1c**, respectively) and enforcing planarity of the two thiophene units as part of a newly formed octatetraene backbone. In comparison with **1.1o**, the extended conjugation pathway established in the ring-closed isomer gives rise to an anodic shift in its reduction potential, as well as an $S_0 \rightarrow S_1$ absorbance band centred in the visible region of the electromagnetic spectrum and an $S_0 \rightarrow S_2$ band positioned in the UV. Either electronic transition can regenerate **1.1o** *via* the reverse reaction (*i.e.* conrotatory cycloreversion), which is often competitive with photochemical ring-formation due to overlap between the $S_0 \rightarrow S_2$ band of **1.1c** with the $S_0 \rightarrow S_1$ band of **1.1o**. The equilibrium composition of the mixture that results from irradiation with UV light is usually expressed as the concentration of **1.1c** divided by the total concentration of both photoisomers and is called the photostationary state. This value is a function of the relative wavelength-dependent quantum yields of ring-opening and ring-

closing, and it is important because it quantifies how effectively the ring-closed isomer can be photochemically generated from its counterpart.[6]

1.2.2 Photodegradation of Dithienylethenes

In many dithienylethenes, including those discussed in Chapter 2 and Chapter 3, photoisomerization is accompanied by irreversible photochemical reactions. In particular, dithienylethenes lacking substituents at the 4- and 4′-positions become incapable of reversible photoisomerization after fewer than 200 cycles, even in the absence of oxygen.[7] Understanding the reaction mechanisms that lead to dithienylethene photodegradation is critical to improving their longevity.

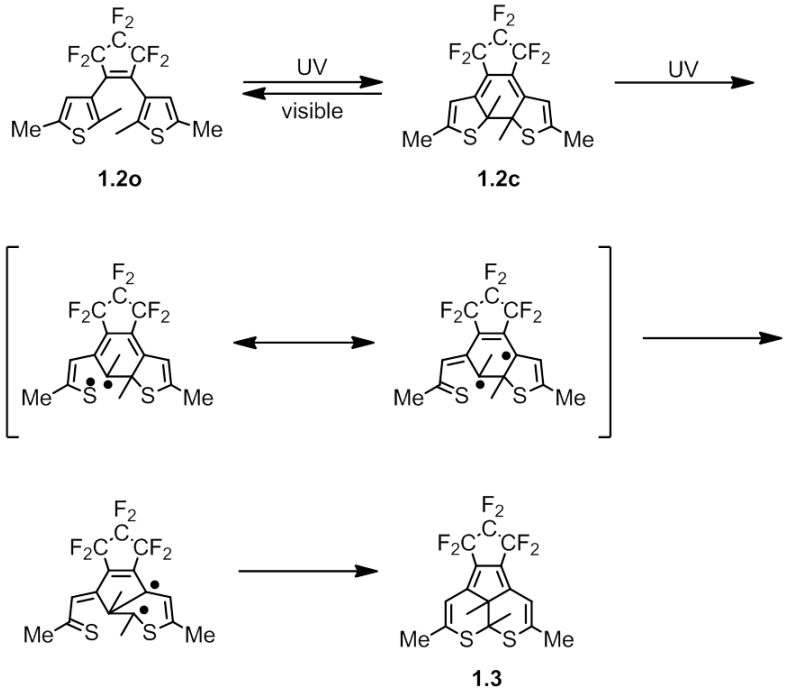

Scheme 1.2 Proposed mechanism for generation of byproduct **1.3** by radical recombination following homolysis of a carbon-sulfur bond.

The mechanism shown in Scheme 1.2 has been proposed in order to explain formation of the major photochemical byproduct, compound **1.3,** during interconversion of dithienylethene isomers **1.2o** and **1.2c**.[8] According to the suggested route, excitation of the ring-closed isomer first leads to homolysis of the bond between sulfur and carbon 2. The resulting sulfur radical is delocalized through the octatetraene backbone, and radical recombination between carbons 2 and 3′ forms a new five-membered ring. This prompts homolysis of the bond between carbons 2′ and 3′, yielding a six-membered ring and another pair of radicals. One of the radicals is delocalized onto the thioketyl sulfur, where subsequent recombination at carbon 2′ produces the second six-membered ring in compound **1.3**. This mechanism is consistent with the significant improvement in fatigue resistance that results from replacing the thiophene rings with benzothiophenes, presumably due to a decrease in radical density at reactive carbons *via* further delocalization onto the benzothiophene backbone. Modifications of this sort allow reversible photoisomerization over more than 14,000 cycles.[9]

These observations are insufficient to explain the improvement in photochemical fatigue resistance that results from having methyl groups at the 4- and 4′-positions on the thiophenes,[5] which should have little effect on the diradical reaction pathway indicated above. Instead, these substituents prevent photochemical generation of byproduct **1.4** (Scheme 1.3), which is thought to occur by pericyclic ring-formation from the *parallel* thiophene rotamer rather than the *anti-parallel* (*i.e.* whereby isomer **1.2c** is generated from **1.2o**).[6] Subsequent abstrac-

tion of a hydrogen radical is prevented by the presence of methyl groups or benzothiophene rings in the aforementioned positions.

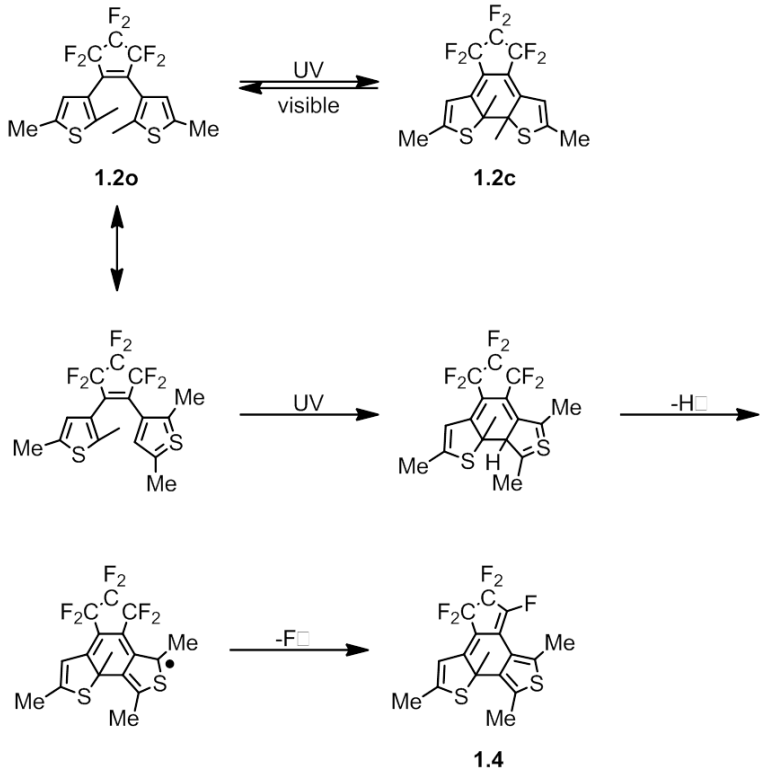

Scheme 1.3 Proposed mechanism depicting formation of byproduct **1.4** by pericyclic ring-formation from the *parallel* thiophene rotamer rather than the *antiparallel* rotamer 1.2o. Subsequent abstraction of hydrogen and fluorine radicals renders the transformation irreversible.

1.2.3 Isomerization in the Dark

In comparison to other photoswitching moieties, the dithienylethene architecture is uniquely resistant to spontaneous isomerization in the absence of light. This feature is important to the photoswitching technologies discussed in Chapters 2 and 3 since the potential for spontaneous interconversion of the two isomers undermines the otherwise strict control over material properties afforded by optical stimuli.

The resistance of dithienylethenes to spontaneous isomerization in the absence of light is due to the reaction taking place *via* concerted pericyclic reactions. When proceeding from the ground state of either dithienylethene isomer, conservation of orbital symmetry requires that these reactions occur by disrotatory mechanisms. In the case of ring formation, this would lead to substituents R^1 and R^2 being positioned *syn* to one another (*i.e.* rather than *anti*, as seen in **1.1c,** in Scheme 1.1). However, R^1 and R^2 are usually alkyl or aryl substituents in order to prevent spontaneous aromatization of **1.1c** *via* oxidation[10] or elimination[11] reactions at those positions, and their steric bulk results in significant activation barriers for either disrotatory pericyclic reaction relative to competing chemical transformations.[12] This is consistent with the observation that in most dithienylethenes the ring-closed isomer persists (>99%) after 12 h at 80° C.[13] Nevertheless, when R^1 and R^2 are excessively bulky (*e.g.* isopropyl groups)[14] or when strongly electron-withdrawing substituents[15] are present on the thiophenes (*e.g.* formyl or cyano groups) spontaneous cycloreversion of the ring-closed isomer is known to occur at elevated temperatures in the absence of light.[16] This reaction is thought to proceed *via* a different mechanistic pathway having diradical character.[17]

1.3 **Photoswitching Motifs Based on Dithienylethenes**

Interconversion of ring-open and ring-closed dithienylethene photoisomers is accompanied by the numerous structural and electronic changes discussed above. The following section highlights several photoswitching technologies in which those changes are harnessed as a means to control other physical or

chemical phenomena using light. In particular, photoswitching motifs based on changes in electronic delocalization are relevant to the system described in Chapter 3 of this thesis, whereas examples of redox photoswitching are relevant to the dithienylethene system described in Chapter 2.

1.3.1 Controlling Electronic Delocalization Between Substituents

The extended conjugation pathway formed during photochemical ring-closure facilitates delocalization of electron density between substituents positioned on different thiophenes; ring-opening ceases delocalization along this pathway. The example shown in Scheme 1.4 illustrates how these changes can be used to control the flow of electrical current between two electrodes bridged by a network of gold nanoparticles. In this system, adjacent nanoparticles are covalently bound to one another by dithienylethene molecules bearing sulfydryl groups at opposite ends. The dithienylethenes facilitate control over charge transport throughout the nanoparticle network by affording varying degrees of electronic delocalization between the bound nanoparticles, depending on which isomer is present. In the case of particles bound by dithienylethene **1.5o**, charge transport is inefficient due to limited overlap among pi orbitals on the benzothiophene and perfluorocyclopentene rings, resulting in only 2 nA of current at an electrical potential of 4 V. Photochemical conversion to compound **1.5c** locks the three rings together in a coplanar arrangement that significantly improves orbital overlap and electronic delocalization across the dithienylethene backbone, allowing superior charge transport between adjacent nanoparticles and generating nearly 30 nA current at the same electrical potential (*i.e.* 4 V).[18]

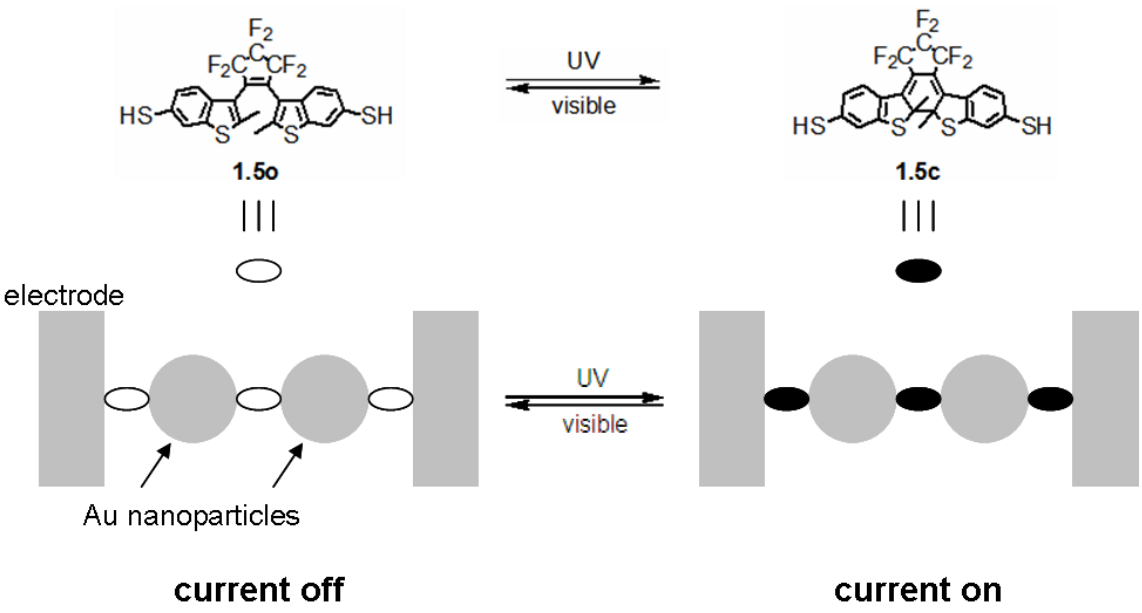

Scheme 1.4 Interconversion of dithienylethene isomers 1.5o and 1.5c regulates the flow of electrical current between two electrodes bridged by a network of covalently bound gold nanoparticles.

An alternate motif exploits changes in orbital hybridization at carbons 2 and 2′ that occur during photoisomerization. The example shown in Scheme 1.5 indicates how this approach can be used to vary the acidity of a phenol substituent at this position. The conjugate base that results from deprotonation of the hydroxyl moiety in compound **1.6o** is stabilized by resonance delocalization of electron density from the phenolate anion onto the methylpyridinium moiety positioned at carbon 5′ on the same thiophene. Irradiation with UV light produces the ring-closed isomer **1.6c**, in which carbon 2 is sp^3 rather than sp^2-hybridized. This prevents resonance delocalization of electron density between the phenolate and pyridinium substituents, and the conjugate base is less stable as a result. Consequently, the ring-open isomer is more acidic than the ring-closed, having a pK_a of 9.8 as opposed to 10.2.[19]

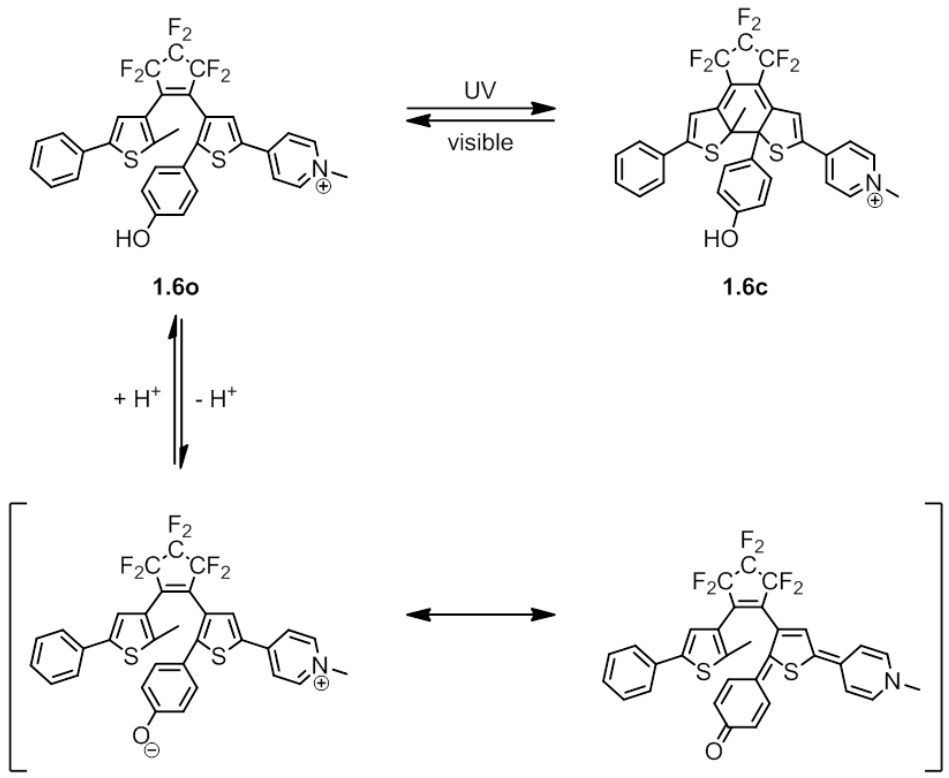

Scheme 1.5 pK_a switching induced by interconversion of **1.6o** and **1.6c** with UV and visible light. The conjugate base of **1.6o**, but not **1.6c**, is stabilized by resonance delocalization of electron density from the phenolate onto the methylpyridinium moiety.

1.3.2 Redox Photoswitching

The changes in redox potentials that accompany interconversion of ring-open and ring-closed dithienylethene photoisomers make it possible to turn “on” or “off” electron transfer reactions between the dithienylethene and a suitable donor or acceptor in close proximity.

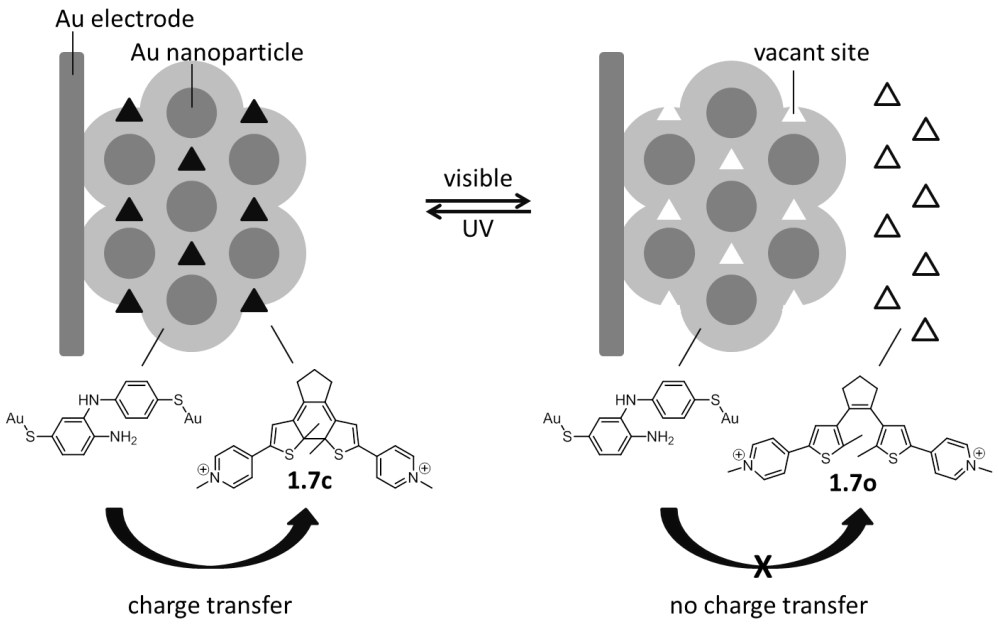

Scheme 1.6 Mercaptoaniline ligands bound to Au nanoparticles are electrochemically dimerized in the presence of **1.7c**, forming a host-guest complex based on charge transfer interactions. Irradiation with visible light generates **1.7o**, which does not participate in charge-transfer and exits the host matrix *via* diffusion. Subsequent irradiation of diffuse **1.7o** with UV light regenerates **1.7c** and stimulates reuptake.

The system shown in Scheme 1.6 depicts how this approach can be used to control the release and reuptake of dithienylethene molecules from a host material. In this example, a host-guest complex is prepared by electrochemical dimerization of mercaptoaniline ligands supported on gold nanoparticles while in the presence of ring-closed **1.7c**. The occurrence of charge transfer interactions between the two species (*i.e.* **1.7c** acts as an electron acceptor and *bis*(mercaptoaniline) acts as a donor) results in the dithienylethene occupying sites embedded in the *bis*(mercaptoaniline) matrix. Conversion of **1.7c** to its corresponding ring-open isomer **1.7o** upon exposure to visible light results in dissociation of the dithienylethene from the *bis*(mercaptoaniline) matrix; afterwards, irradiation of diffuse **1.7o** with UV light regenerates the ring-closed isomer **1.7c**

and stimulates its reuptake. This behavior is attributable to manipulation of the charge transfer interactions responsible for attraction between the two species and is consistent with differences in the reduction potentials of the dithienylethene photoisomers (*i.e.* -1.1 V *vs.* saturated calomel electrode (SCE) in **1.7o**, as opposed to -0.42 V *vs.* SCE in **1.7c**). It is also supported by the fact that electrochemical reduction of the *bis*(mercaptoaniline) matrix results in dissociation of **1.7c**.[20]

A second example of redox photoswitching is depicted in Scheme 1.7, in which interconversion of ring-open and ring-closed dithienylethene photoisomers is used to modulate the flow of electrical current in a macromolecular assembly. In this example, hexabenzocoronenes covalently modified with dithienylethene **1.8o** spontaneously self-assemble into photoconductive, tubular nanostructures; selective photoexcitation of the hexabenzocoronene layer under an applied electric potential leads to the generation of photocurrent (*i.e.* +0.03 nA at +2 V). Conversion of dithienylethene **1.8o** to its corresponding ring-closed isomer **1.8c** *via* irradiation with UV light results in a fivefold increase in photocurrent generated by the nanotubes under the same conditions (*i.e.* +0.15 nA at +2 V). This is due to the anodic shift in the reduction potential of the dithienylethene as it is converted to the ring-closed isomer (*i.e.* the reduction potential of **1.8o** is -2.4 V *vs.* SCE, and the reduction potential of **1.8c** is -1.0 V *vs.* SCE), which increases the efficiency of photoinduced electron transfer from the hexabenzocoronene to the dithienylethene moiety and improves charge carrier generation.

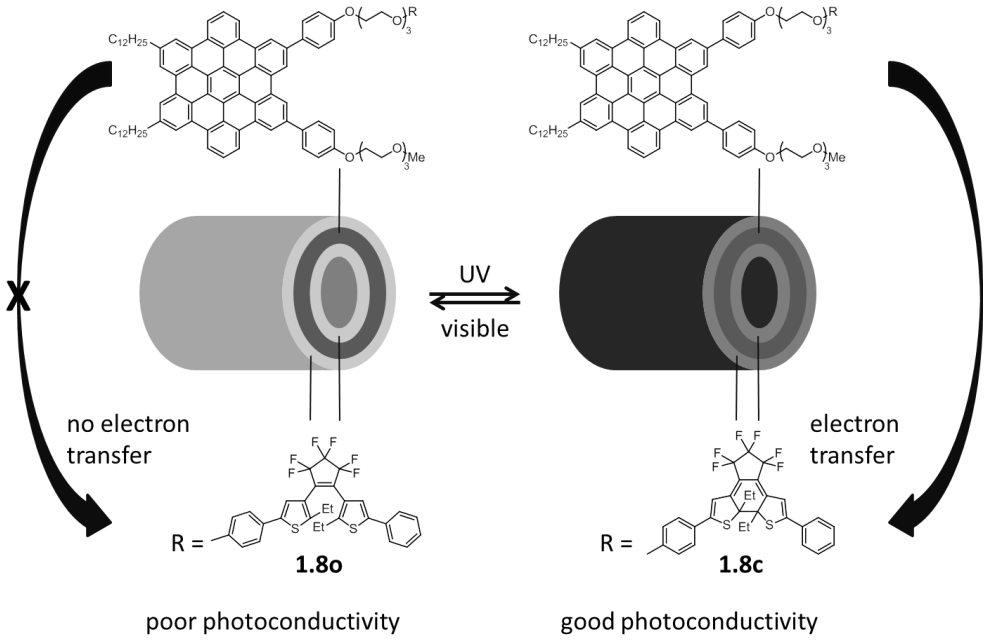

Scheme 1.7 Dithienylethene-modified hexabenzocoronenes **1.8o** spontaneously assemble into tubular nanostructures that exhibit poor photoconductivity. Irradiation of the nanotubes with UV light results in conversion of the dithienylethene unit to isomer **1.8c**, which results in a fivefold growth in photoconductivity *via* improved charge-carrier generation as a result of intramolecular electron transfer.

1.4 **Summary and Thesis Overview**

In this chapter, optical stimuli are highlighted as an excellent means to selectively manipulate the behavior of individual components in a mixture. Photoswitching motifs are discussed as a means to simplify the design of photoresponsive systems by affording a molecular architecture whose physical and chemical properties can be reversibly toggled between two states using light of different wavelengths. In particular, the dynamic structural features of dithienylethene photoswitches are addressed, as are methods of harnessing them for photochemical modulation of surrounding materials in ways that potentially impact molecular electronics, catalysis, and biochemical sensing technologies.

In Chapter 2 controllable luminescent materials are introduced as valuable tools for sensing, imaging and data storage applications. Methods of regulating light emission are generalized based on changes to a recurring quencher-lumophore motif, with special emphasis placed on switchable dithienylethene quenchers. In order to address the shortcomings of previous designs, a new quencher-lumophore assembly is proposed in which quantum dot (QD) luminescence is reversibly controlled by photoisomerization of a cationic dithienylethene coordinated to the QD surface. The synthesis of the complex is discussed, as are spectroscopic and electrochemical studies intended to assess its performance with regard to luminescence quenching.

In Chapter 3 several promising technologies that utilize thermoresponsive materials are highlighted, particularly those based on Diels-Alder (DA) reaction equilibria. The ability to control thermoresponsive systems using light is suggested as a means to extend their benefits to a wider range of working environments by offering a means to mitigate unintended effects arising from circumstantial or otherwise unavoidable exposure to temperatures outside the desired regime. The construction of molecular photoswitches using the DA reaction is proposed as a motif to facilitate optical regulation of thermoresponsive materials. The syntheses of three dithienylfuran compounds are described, as well as subsequent efforts to screen them based on adduct formation with different dienophiles. Also addressed are the photochemical properties of the adducts and, in one compound, the ability to reversibly toggle thermoresponsive behavior using light is discussed.

CHAPTER 2: CONTROLLING LUMINESCENT MATERIALS WITH MOLECULAR SWITCHING

2.1 Quencher-Lumophore Assemblies

2.1.1 Introduction

The extraordinary sensitivity of luminescence measurements and the responsiveness of light-emitting materials to optical stimuli (*i.e.* during excitation) have found great utility in imaging technologies. The ability to control luminescent materials using a second set of stimuli conveys additional benefits that extend their usefulness to sensing and data storage applications. This is commonly accomplished by design motifs in which a light-emitting material (lumophore) is paired with a second component (quencher) that, under certain conditions, enables radiationless deactivation of the lumophore excited state, usually *via* Förster Resonance Energy Transfer (FRET) or photoinduced electron transfer.

In FRET, through-space transfer of the lumophore (*i.e.* donor) excitation energy to the ground-state quencher (*i.e.* acceptor) occurs through a dipole-dipole interaction between the two moieties; this returns the donor to its ground state (*i.e.* without emission) and generates the excited state of the acceptor.[21] In photoinduced electron transfer, an electron can be transferred from the excited lumophore to the quencher LUMO, or an electron can be transferred from the quencher HOMO to the lower-energy, singly-occupied molecular orbital of the

quencher; both types of transfer occur through space and result in radiationless deactivation of the lumophore excited state.[22]

By using a second stimulus to vary the conditions that dictate the efficiencies of those processes, it is possible to control whether an excited lumophore will emit light.

2.1.2 Varying Quencher-Lumophore Separation

The inverse distance dependence of luminescence quenching efficiency by a suitable FRET acceptor or electron transfer partner can be harnessed by using a second stimulus to increase or decrease the separation between lumophore and quencher, turning luminescence “off” or “on”, respectively.

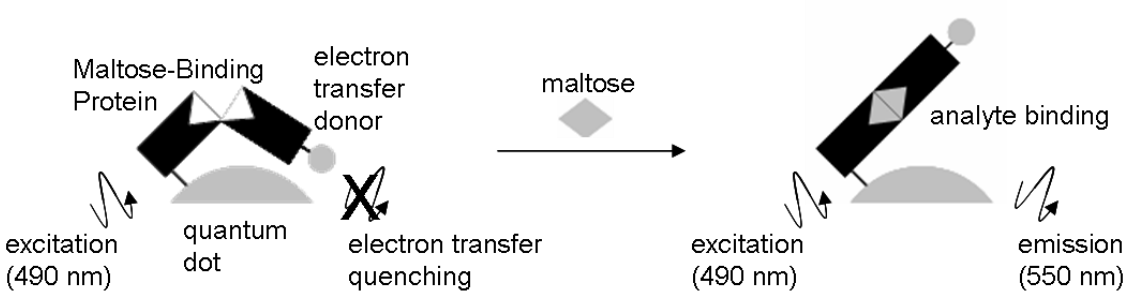

Scheme 2.1 A maltose chemosensor based on amplification of QD luminescence resulting from analyte recognition by maltose-binding Protein (MBP), which is accompanied by a change in protein conformation that increases the separation between an electron transfer donor and the QD surface.

The example shown in Scheme 2.1 demonstrates this approach applied to the detection of maltose. In the absence of analyte, quantum dot (QD) light emission is quenched by an electron transfer donor covalently bound to a maltose-binding protein (MBP) molecule immobilized on the particle surface. The binding of maltose to MBP induces a change in protein conformation that distances the

electron transfer donor from the QD surface, decreasing the efficiency of luminescence quenching. In this manner, maltose detection is signalled by an increase in QD light emission.[23]

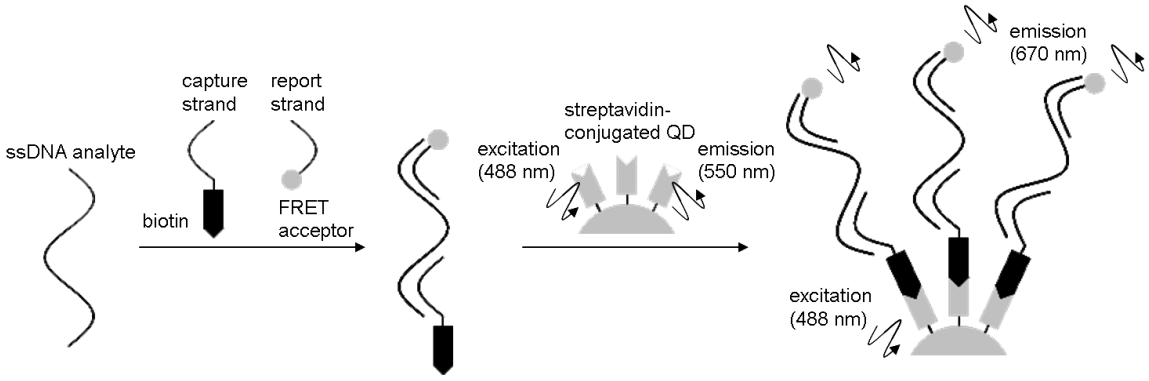

Scheme 2.2 Multiplex segment recognition of analyte ssDNA sequence by a report strand (bearing a FRET acceptor) and a capture strand (carrying a biotin label) facilitates binding to a streptavidin-conjugated QD, resulting in light emission from the FRET acceptor during excitation of the QD.

Another example, shown in Scheme 2.2, highlights the utility of chemically gated luminescence for sequence-specific detection of biomolecules like DNA. Here, detection of an ssDNA analyte is signalled by enhancement of 670 nm light emission from a FRET acceptor during 488 nm excitation of a QD, which acts as a donor; in the absence of analyte, QD emission at 550 nm is observed instead. The FRET acceptor is covalently bound to a “report strand,” a shorter ssDNA segment capable of complementary base pairing to one end of the analyte. Complementary pairing between the other end of the analyte and a biotinylated “capture strand” ultimately brings the FRET acceptor into close proximity with the streptavidin-functionalized QD and enhances FRET efficiency, signalling the presence of analyte.[24]

2.1.3 Modifying the Quencher

Another approach to controlling light-emitting materials is to use a second stimulus (*i.e.* in addition to optical excitation of the lumophore) to alter the quencher frontier molecular orbitals (FMOs) in a manner that converts it from an effective FRET or electron transfer partner (quencher 2) into a poor one (quencher 1), or *vice versa* (Figure 2.1). Efficient FRET requires that the lumophore (donor) and quencher (acceptor) have similar energetic HOMO-LUMO separations, which are experimentally quantifiable by examining spectral overlap between the emission band of the lumophore and the absorption band of the quencher; since $\Delta E_{Q1} > \Delta E_L \approx \Delta E_{Q2}$ it is likely that FRET from the lumophore to quencher 2 will be effective, but FRET from the lumophore to quencher 1 will not. On the other hand, the efficiency of photoinduced electron transfer depends on whether the quencher acts as a donor or as an acceptor of an electron: as a donor, electron transfer from the quencher is favoured when its HOMO is higher in energy than the lumophore HOMO, a condition that is not met for either quencher 1 or quencher 2; as an acceptor, electron transfer to the quencher is favoured when its LUMO is lower in energy than the lumophore LUMO, a condition met in quencher 2 but not quencher 1.

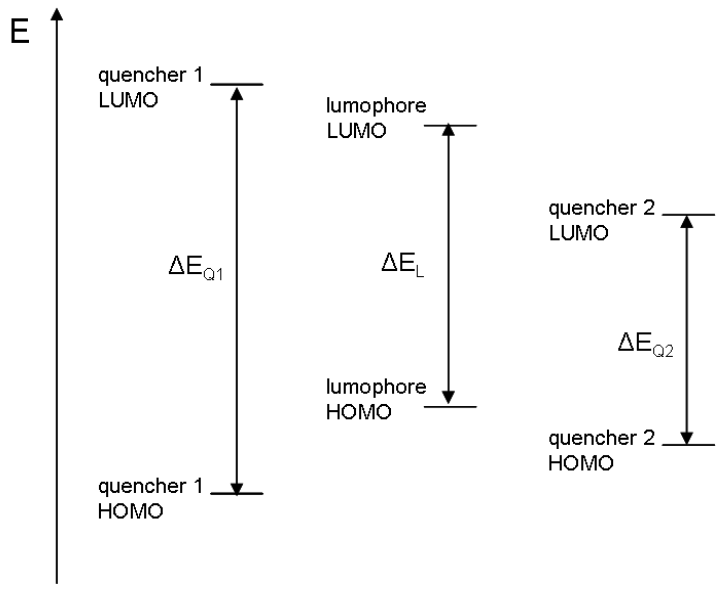

Figure 2.1 Frontier orbital energy diagram for a lumophore and two possible quenchers. ΔE_L, ΔE_{Q1} and ΔE_{Q2} represent the HOMO-LUMO separations for the lumophore, quencher 1 and quencher 2, respectively.

The use of optical stimuli to modify the quencher is attractive for prospective data storage and super-resolution microscopy techniques. In the former, data is recorded in the form of the binary on/off state of the quencher that results from photochemical transformations analogous to “write” and “erase” operations; data is “read” by electronically exciting the lumophore and interpreted digitally based on whether or not light is emitted. Super-resolution imaging techniques like stimulated emission depletion (STED) microscopy, on the other hand, harness on/off control of luminescent materials to spatially confine emission from excited lumophores, resulting in image resolution that transcends the optical diffraction limit (Figure 2.2).[25]

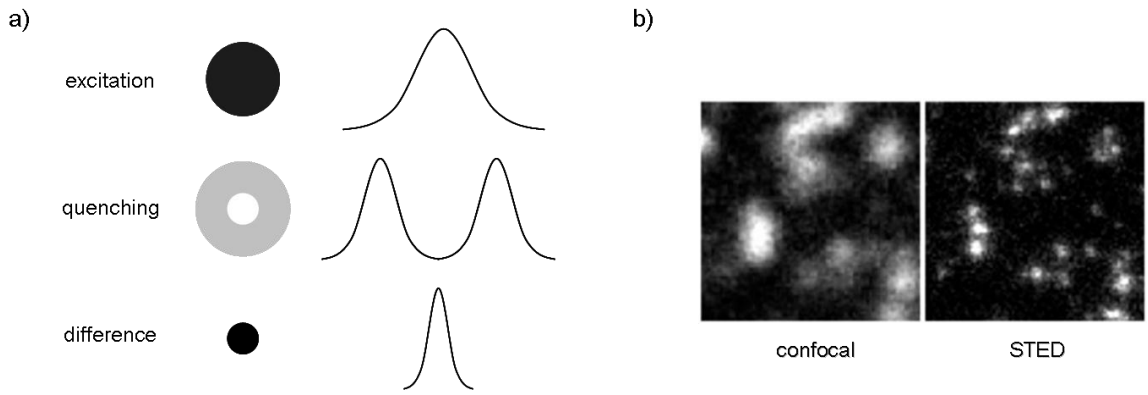

Figure 2.2 (a) Stimulated Emission Depletion (STED) microscopy utilizes a quenching beam whose cross section contains a circular zero-intensity region in the centre to spatially confine emission from lumophores excited using a second beam. (b) Confocal and STED microscopy images acquired from DNA replication centres in cellular nuclei (Ref. 25, reprinted with permission from the authors).

Molecular switching motifs are well-suited to this paradigm, providing a convenient and reliable means of toggling quencher FMO energies. For instance, the increase in visible light absorption that accompanies dithienylethene ring-closure can be harnessed as a means to improve spectral overlap with the lumophore and thus enhance luminescence quenching *via* FRET (assuming the luminescent donor and switch acceptor are sufficiently close to one another). This approach is demonstrated by the example shown in Scheme 2.3, in which QD luminescence is photochemically gated by interconversion of dithienylethene isomers bound to the lumophore surface by a biotin-streptavidin linker. The ring-open dithienylethene photoisomer in **2.1o** has an absorption band centred in the UV, which overlaps poorly with the QD emission band (centred at 565 nm) and results in inefficient FRET as a means of luminescence quenching. Irradiation with UV light generates the ring-closed photoisomer in **2.1c**, which has an absorbance maximum centred at 555 nm. Improved spectral overlap between do-

nor (the QD) and acceptor (the ring-closed dithienylethene) yields efficient FRET and suppresses light emission from the complex.[26] A common shortcoming of this methodology is that FRET-based quenching results in electronic excitation of the ring-closed dithienylethene isomer, which can lead to a gradual decrease in donor-acceptor spectral overlap and a loss of FRET efficiency as the ring-closed molecule is converted to its ring-open photoisomer (depending on the quantum yield of photochemical ring-opening relative to the combined yields of other radiationless deactivation pathways).

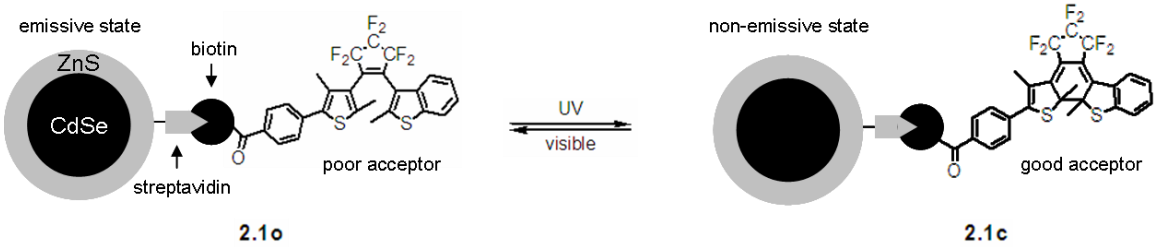

Scheme 2.3 Luminescence from a streptavidin-conjugated quantum dot reversibly quenched by interconversion of biotinylated dithienylethene ring-open and ring-closed photoisomers. The ring-closed isomer **2.2c** is a good FRET acceptor; the ring-open isomer **2.2o** is not.

An alternative approach is to harness the changes in redox properties that accompany dithienylethene isomerization as a means of suppressing and activating photoinduced electron transfer pathways. This method circumvents the limitations associated with FRET-based quenching because it does not result in electronic excitation of the dithienylethene, though care must be taken to ensure that the ensuing radicals recombine rapidly rather than reacting further. The example shown in Scheme 2.4 highlights this approach, employing ring-open and ring-closed dithienylethenes covalently bound to a luminescent perylenebisimide

component that emits light at wavelengths in the near-IR when excited with 700 nm light. Quenching *via* FRET is unlikely to take place in either photoisomer since the longest wavelength absorption maxima for the ring-open and ring-closed moieties occur in the UV and visible spectral regions, respectively, which result in poor spectral overlap between donor and acceptor. However, by comparing the reduction potentials of the ring-open and ring-closed dithienylethene moieties in compounds **2.2o** and **2.2c** (< -2.00 V in the former, +1.00 V in the latter, both *vs.* Fc / Fc+) with the oxidation potential and absorption maximum of the perylenebisimide component (+0.22 V *vs.* Fc / Fc+, 700 nm) it is evident that the perylenebisimide LUMO lies energetically below that of the ring-open dithienylethene and above that of the ring-closed. This suggests that luminescence from the perylenebisimide moiety should be effectively quenched by electron transfer to the ring-closed dithienylethene but not the ring-open. Indeed, transient absorption measurements verify that the $S_1 \rightarrow S_0$ lifetime of the perylenebisimide component is shortened from 1.5 ns in **2.2o** to 230 ps in **2.2c**, indicating competitive deactivation of the luminescent excited state in the latter.[27]

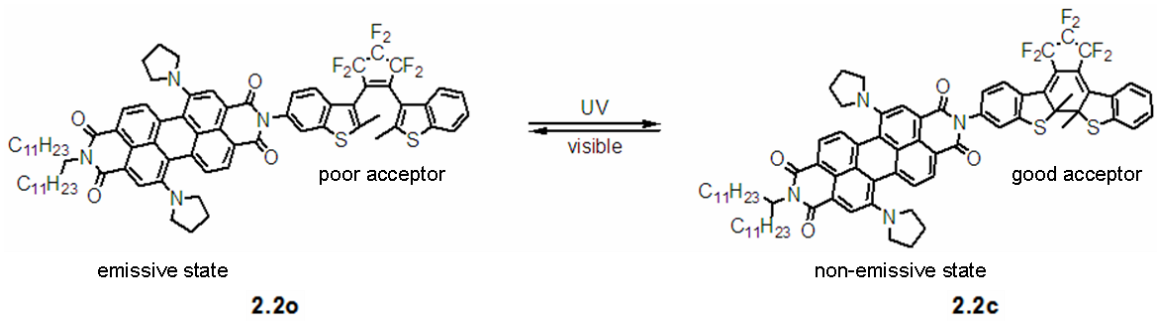

Scheme 2.4 Intramolecular modulation of fluorescence from perylenebisimide by photoisomerization of the covalently bound dithienylethene moiety.

2.2 Designing an Optimized Quencher-Lumophore Assembly

2.2.1 Lumophore Optimization

In both FRET and electron transfer quenching, a switchable quencher is best complemented by a lumophore having narrow, tunable emission and a long luminescent lifetime. QDs perform well in both regards, having emission bands that can be tuned throughout the visible and near-IR as a function of particle size,[28] as well as luminescence lifetimes nearly five times greater than archetypal organic fluorophores (Table 2.1).[29] In addition, they are relatively resistant to photo-bleaching[30] and have continuously high molar extinction coefficients across much of the UV and visible spectral regions, allowing selective excitation of the QD even in the presence of a switchable quencher or other chromophores.

Table 2.1 Emission parameters of common lumophores.

	ε_A[a] / $mM^{-1}\,cm^{-1}$	σ[b] / GM	$\Delta\lambda$[c] / nm	Φ_F[d]	τ_F[e] / ns
Fluorescein	83	54	44	0.93	4.0
Oregon Green 488	81	—	58	0.90	4.1
Cy3	150	—	50	0.15	0.2
Rhodamine 6G	95	6	45	0.95	4.1
Texas Red	116	—	37	0.54	4.2
Cy5	250	400	40	0.28	2.1
CdSe-ZnS Quantum Dots[f]	98	47,000	31	0.28	17.1

[a] Molar extinction coefficients at λ_{ex}. [b] Two-photon absorption cross-sections of fluorescein at 800 nm, of Rhodamine 6G at 798 nm, of Cy5 at 820 nm and of the quantum dots at 900 nm. [c] Width of emission bands at half-maximum. [d] Quantum yields. [e] Fluorescence lifetimes. [f] Values indicated are for CdSe-ZnS quantum dots in which the diameter of the CdSe core is approximately 2.9 nm. (Ref. 29)

QDs are equally versatile from a synthetic perspective, as their surfaces are amenable to a variety of bond-forming chemistries (Scheme 2.5). A typical approach is to first replace the trioctylphosphine oxide (TOPO) stabilizer (a common remnant among micellar QD preparation methods) with ligands bearing atoms or functional groups capable of stronger coordination to the surface of the insulating QD shell (*e.g.* thiols, amines, hydroxides, carboxylates, *etc*.) Depending on the chemical properties of the solvent-facing end of the ligand, further modifications are possible *via* ionic binding, receptor-affinity binding or covalent coupling reactions[31] that allow tailoring of the QD surface to the specific demands of numerous applications.[32]

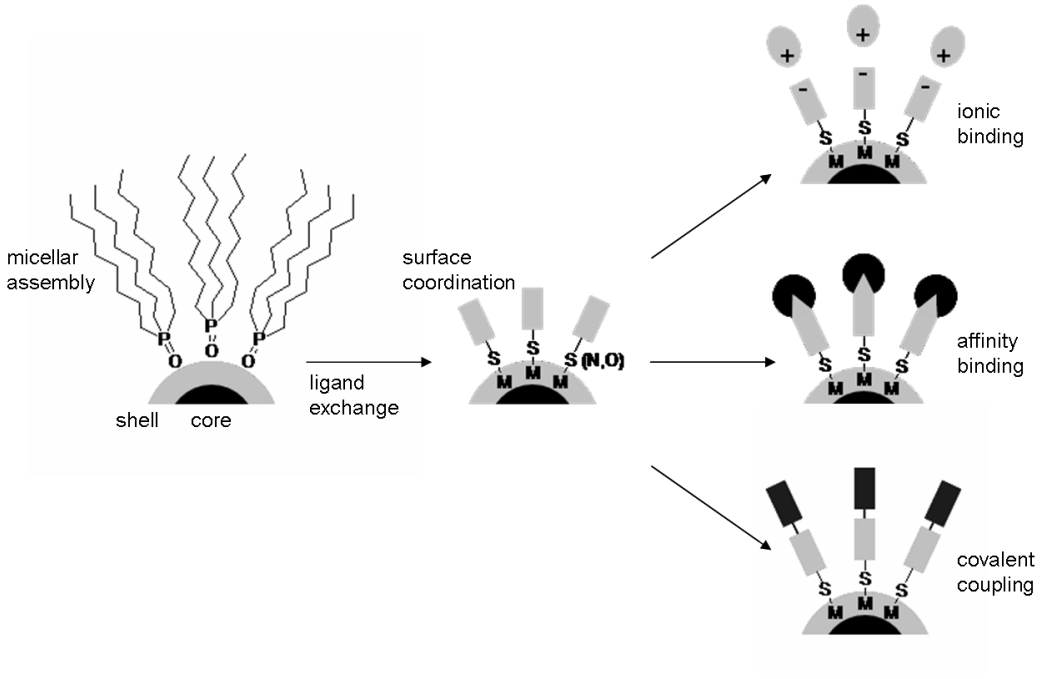

Scheme 2.5 Strategies for surface functionalization of core-shell QDs.

2.2.2 Quencher Optimization

To date there have been only a handful of reported molecular switch-QD assemblies enabling optical control of luminescence, including the examples shown in Scheme 2.3 and Scheme 2.6.[33] Most employ spiropyran molecules as switchable FRET acceptors anchored to the QD by lengthy protein or alkanethiol appendages.[34,35] These designs share some common weaknesses: the weaknesses associated with FRET-based quenching have already been discussed; additionally, attachment to the QD surface *via* an intervening ligand is also problematic as it significantly increases the synthetic complexity of the system and lowers FRET and electron transfer rates due to increased quencher-lumophore separation; finally, conversion of the colourless spiropyran to its coloured isomer using UV light is often spontaneously reversible under ambient conditions even in the absence of light (as is the case for regeneration of compound **2.3s** from **2.3m**), causing unprompted loss of quenching efficiency in the quencher-lumophore complex.

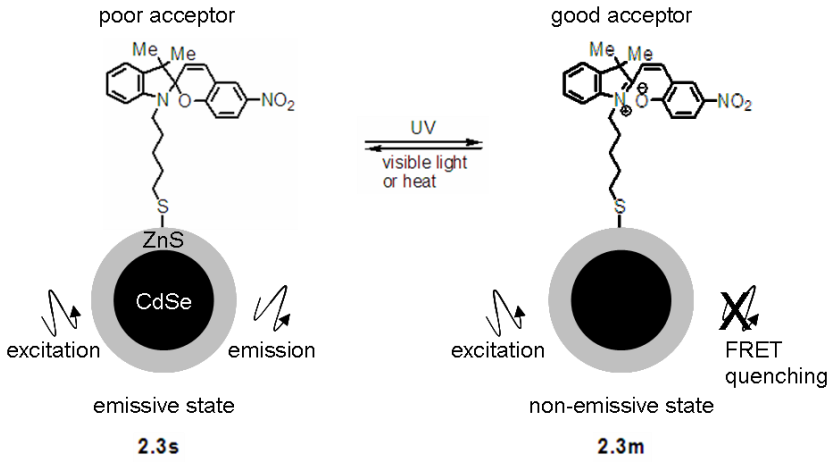

Scheme 2.6 Reversible FRET-based quenching of QD luminescence by interconversion of colourless spiropyran **2.3s** and coloured merocyanine **2.3m** using UV and visible light or heat.

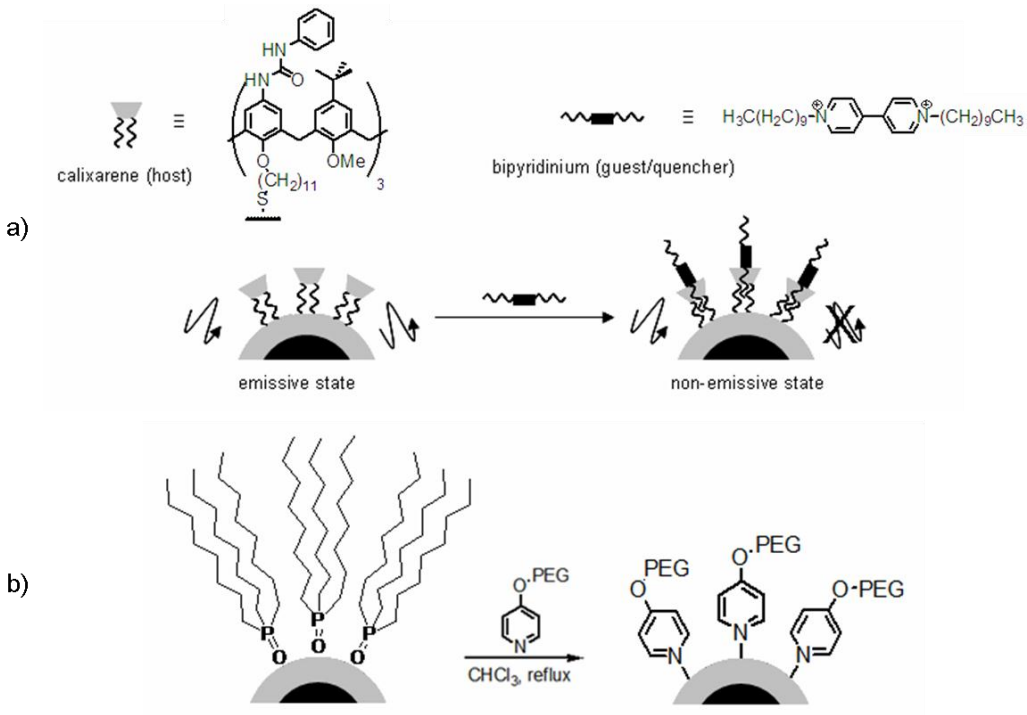

Scheme 2.7 (a) Host-guest interactions between bipyridinium cations and calixarenes bound to QDs leads to quenching of QD luminescence by electron transfer. (b) Surface modification of QDs with poly(ethylene)glycol (PEG)-derivatized pyridine molecules *via* ligand exchange.

The first of these shortcomings can be remedied by employing a switching architecture in which the change in redox properties that accompanies photoisomerization (as opposed to the change in optical absorbance) quenches or restores luminescence by activating or deactivating an electron transfer pathway. Reports of QD luminescence quenching by electron transfer to bipyridinium cations (Scheme 2.7a) suggest that this structural motif could be useful in designing an appropriate switch.[36] The second problem can be solved by incorporating into the molecular switch a functional group that facilitates direct attachment to the QD surface. Strong sigma-donor ligands like *para*-substituted pyridines have been found to perform well in this regard (Scheme 2.7b).[37] The third solution is to

use dithienylethenes as switching components (rather than spiropyrans) since their coloured ring-closed forms do not undergo spontaneous isomerization in the dark except at elevated temperatures, nor are they susceptible to the dark, solvent-driven degradation reactions that plague spiropyrans.[38]

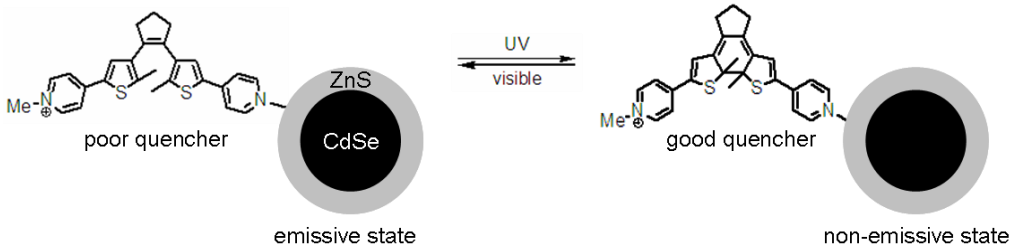

Scheme 2.8 Photoisomerization of a dithienylethene bearing pyridine and alkyl pyridinium functional groups as a means to reversibly quench luminescence from a surface-coordinated core-shell QD.

Based on these constraints, a dithienylethene compound bearing pyridine and alkylpyridinium functional groups was designed in order to facilitate direct binding to the QD surface and reversible quenching of QD luminescence *via* electron transfer to the ring-closed isomer but not the ring-open (Scheme 2.8). The synthesis of both molecular switch isomers and the subsequent attachment of the ring-closed compound to core-shell QDs are explained in the following section; later sections address spectral evidence for photoisomerization of the dithienylethene on and off the QD surface, as well as data demonstrating that the two isomers quench QD luminescence to differing degrees. These differences are then rationalized in terms of FRET and electron transfer mechanisms based on spectral and electrochemical measurements acquired from the unbound dithienylethene isomers.[39]

2.3 **Results and Discussion**

2.3.1 Synthesis

2.3.1.1 Dithienylethene Quencher

Compound **2.8** was synthesized from commercially available materials using established literature procedures (Scheme 2.9), beginning with regioselective chlorination of 2-methylthiophene to produce compound **2.5**. Acylation of compound **2.5** with one-half equivalent of glutaryl chloride generated diketone **2.6**, which was then cyclized *via* intramolecular McMurry coupling of the two carbonyl groups to furnish cyclopentene **2.7** in modest yield.[40] Lithium-halogen exchange followed by treatment with *tris*-(*n*-butyl)borate afforded the dithienylcyclopentene *bis*(boronic acid) ester, which was not isolated; rather, Suzuki cross-coupling of the crude product with 4-bromopyridine hydrochloride led to formation of *bis*(pyridine) **2.8** in excellent yields.[41] Alkylation of compound **2.8** with one equivalent of methyl iodide afforded dithienylethene monocation **2.9o**, which underwent photochemical ring-closure upon irradiation with 313 nm light to form isomer **2.9c**. Neither compound **2.9o** nor **2.9c** has been previously reported.

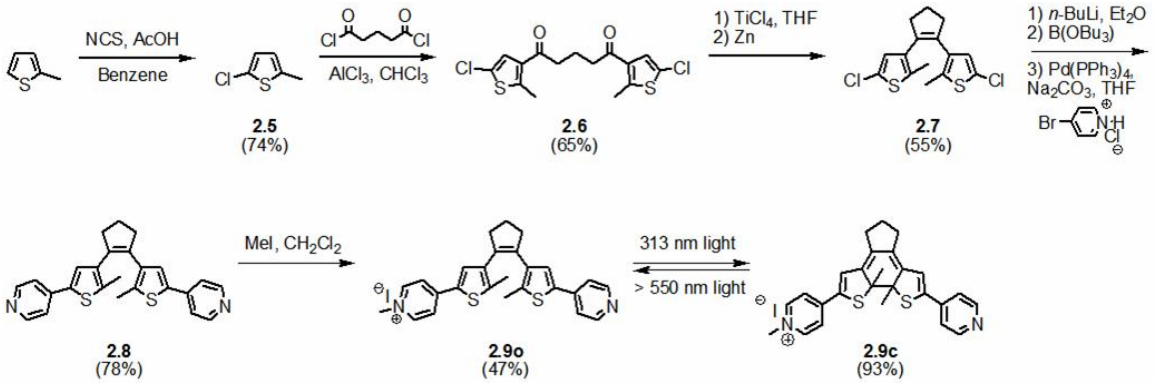

Scheme 2.9 Synthesis of ring-closed dithienylethene **2.9c.**

2.3.1.2 QD Functionalization

A crude mixture of dithienylethenes **2.9c** and **2.9o** (93:7) was attached to 5.6 nm CdSe-ZnS QDs (**QD•TOPO**) *via* ligand exchange in refluxing chloroform, yielding the target quencher-lumophore complex **2.9c•QD** (Scheme 2.10). However, purification of the complex was complicated by noteworthy material losses due to incomplete resuspension of the decorated QDs in fresh solvent following centrifugation, suggesting decreased particle stability as a result of ligand exchange.

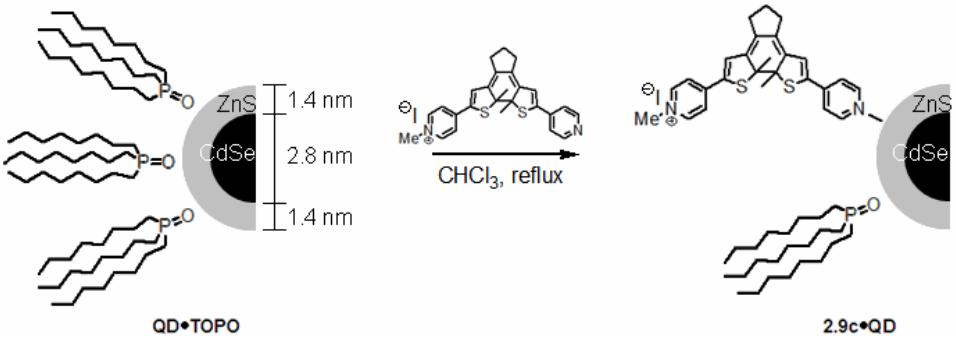

Scheme 2.10 Preparation of molecular switch-quantum dot complex **2.9c•QD** from TOPO-capped, 5.6 nm CdSe-ZnS quantum dots (**QD•TOPO**) by ligand exchange.

2.3.2 Absorbance and Redox Photoswitching

Photochemical formation of dithienylethene **2.9c** from its corresponding ring-open isomer **2.9o** was monitored by UV-vis absorbance spectroscopy prior to QD complex formation (Figure 2.3). Irradiation of a solution containing the ring-open isomer (*i.e.* with 313 nm light) led to a decrease in absorbance between 250 nm and 300 nm as the concentration of compound **2.9o** decreased. Meanwhile, the absorbance between 380 nm to 400 nm increased and a new absorbance band formed in the visible region of the spectrum, centred at 671 nm, con-

sistent with formation of the ring-closed isomer **2.9c** (see Section 1.2.1). The photostationary state (*i.e.* PSS_{313}) was determined *via* ^{1}H NMR spectroscopy and found to consist of approximately 93% ring-closed isomer **2.9c** (see Section 2.5.5 for spectral characterization of each isomer).

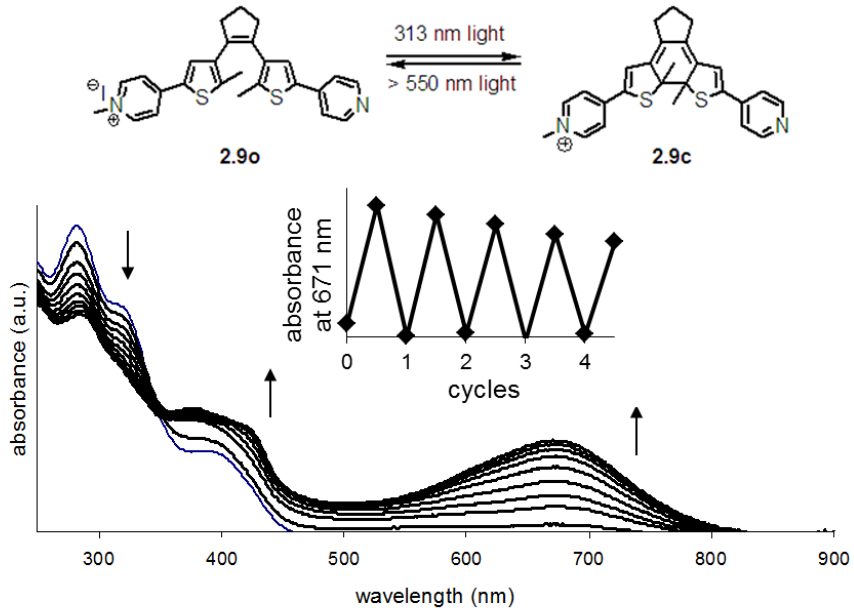

Figure 2.3 UV-vis absorbance spectra of a $CHCl_3$ solution containing compound **2.9o** (1 x 10^{-5} M, 20 °C) acquired during exposure to 313 nm light in 5 s intervals; arrows indicate the direction of spectral evolution during UV exposure. The inset depicts changes in absorbance of the same solution monitored at 671 nm during alternating periods of irradiation with UV (313 nm, 30 s) and visible light (>550 nm, 150 s).

The reversibility of the ring-closing reaction and the resistance of the two dithienylethene isomers to photochemical fatigue were examined by measuring changes in absorbance at 671 nm (corresponding to the visible wavelength absorption band of **2.9c**) during repeated cycling between the two isomers (Figure 2.3, inset). In each cycle, a solution of compound **2.9o** ($CHCl_3$, 1 x 10^{-5} M, 20 °C) was exposed to UV (313 nm, 30 s) and then visible light (>550 nm, 150 s). Ab-

sorbance measurements acquired at 671 nm after each period of irradiation reveal alternating high and low values corresponding to the minimum and maximum concentrations of **2.9c** present, which confirms that photoisomerization is reversible in this system. However, a slight decrease in the maximum absorbance values measured over four cycles indicates a corresponding, cumulative decrease in the amount of **2.9c** present, which suggests that competing, irreversible side reactions occur during photoisomerization (see Section 1.2.2).

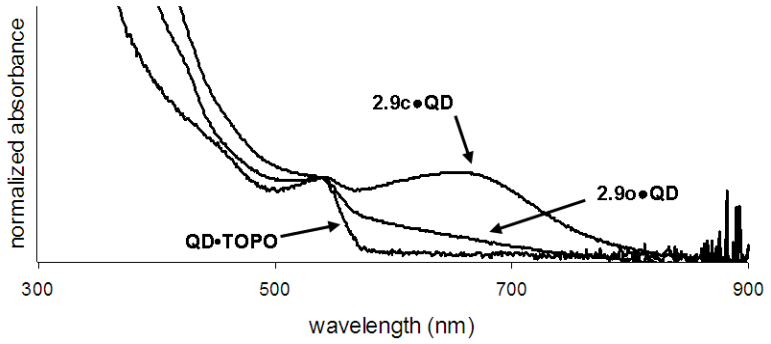

Figure 2.4 Absorbance spectra obtained from **QD•TOPO** and **2.9c•QD** in $CHCl_3$ ($1x10^{-6}$ M, 20 °C). The spectrum labeled **2.9o•QD** was acquired from the solution containing **2.9c•QD** after irradiating it with >550 nm light for 150 s.

UV-vis absorbance spectra were obtained from **QD•TOPO** before and after treatment with compound **2.9c** in order to determine whether ligand exchange took place and whether the dithienylethene can be made to undergo photoisomerization on the QD surface (Figure 2.4). Both the QD absorption band at 530 nm and the 670 nm absorption from the ring-closed dithienylethene are present in the spectrum despite repeated washings with CH_3CN, suggesting that formation of complex **2.9c•QD** was successful (*i.e.* **2.9c** is soluble in CH_3CN but **QD•TOPO** is not). Moreover, the presence of both bands indicates that the excited states of

the QD and the switch remain distinct from one another; this feature is necessary for retention of the separate photochemical (*i.e.* isomerization) and photophysical (*i.e.* luminescence) relaxation pathways of the individual components. Assuming that the molar extinction coefficients of both components remain the same after complex formation, absorbance values at 530 nm and 670 nm indicate three to four dithienylethene molecules are present per QD.

Irradiation of **2.9c•QD** with visible light leads to a decrease in absorbance between 600 nm to 700 nm, which suggests formation of the ring-open dithienylethene isomer on the QD surface (**2.9o•QD**). Attempts to accurately measure the changes in absorbance at 671 nm while cycling between the ring-open and ring-closed dithienylethene isomers (analogous to measurements carried out with compounds **2.9o** and **2.9c** prior to complexation) were thwarted by a steady increase in light scattering, evident as a slanted "shoulder" on the right side of the QD absorbance band centred at 530 nm; this can be attributed to formation of insoluble QD aggregates. Similar problems arose during attempts to prepare samples of the decorated QDs having concentrations suitable for NMR spectroscopy, making it impossible to determine whether the photostationary state of the surface-bound dithienylethene differs from its unbound state. These observations are consistent with the material losses that took place during isolation of the QD complex, which indicate decreased particle stability following exchange of trioctylphosphine oxide (TOPO) for the dithienylethene ligand.

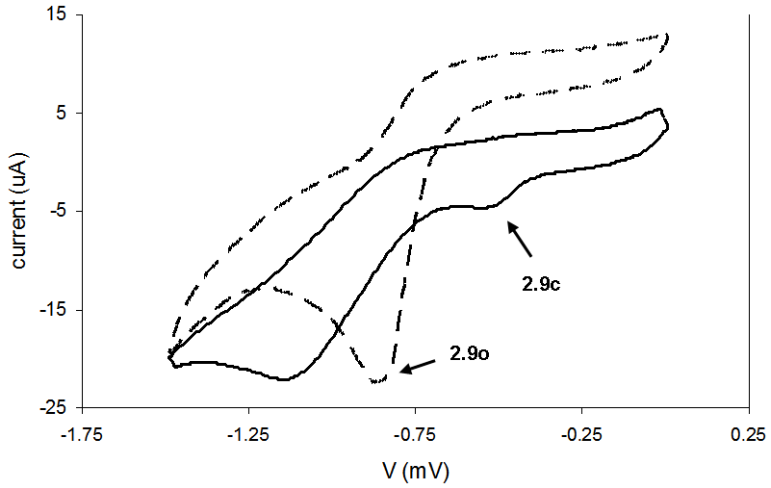

Figure 2.5 Cyclic voltammograms obtained from compounds **2.9o** and **2.9c** in MeCN (1.0 mM, 0.1 M Bu_4NPF_6, 200 mV s^{-1}) referenced to SCE using the ferrocene couple (+475 mV *vs.* SCE) as an internal standard.

The effects of photoisomerization on the electrochemical properties of dithienylethenes **2.9o** and **2.9c** were studied using cyclic voltammetry (Figure 2.5); electrochemical analyses of the corresponding complexes **2.9o•QD** and **2.9c•QD** could not be carried out due to irreversible formation of insoluble aggregates at concentrations needed for cyclic voltammetry experiments. The reduction wave of the ring-open monocation **2.9o** appears at a potential of -0.88 V *vs.* SCE, and photochemical ring-closure results in an anodic shift of +220 mV relative to the reduction potential of the ring-open isomer. The complementary oxidation waves are diminutive in both cases, indicating that the neutral radicals arising from reduction are chemically consumed prior to the anodic sweeps of the potentiostat. The reported stability of the analogous methyl viologen radical under comparable measurement conditions suggests that the reduced forms of

compounds **2.9o** and **2.9c** react in ways peculiar to the dithienylethene architecture.[42]

2.3.3 Luminescence Quenching

QD luminescence is noticeably altered by coordination of compound **2.9c** (Figure 2.6). Light emission from complex **2.9c•QD** is only 4% of the amount emitted by **QD•TOPO**, suggesting efficient quenching by the ring-closed dithienylethene isomer. Irradiation of **2.9c•QD** with visible light (>550 nm) to generate the bound ring-open isomer **2.9o•QD** resulted in a threefold increase in luminescence intensity, but complete recovery of light emission (*i.e.* relative to **QD•TOPO**) was unobtainable, suggesting luminescence quenching by the ring-open isomer as well. Subsequently, exposure of **2.9o•QD** to UV light (313 nm) regenerated **2.9c•QD** and restored quenching efficiency (Figure 2.7).

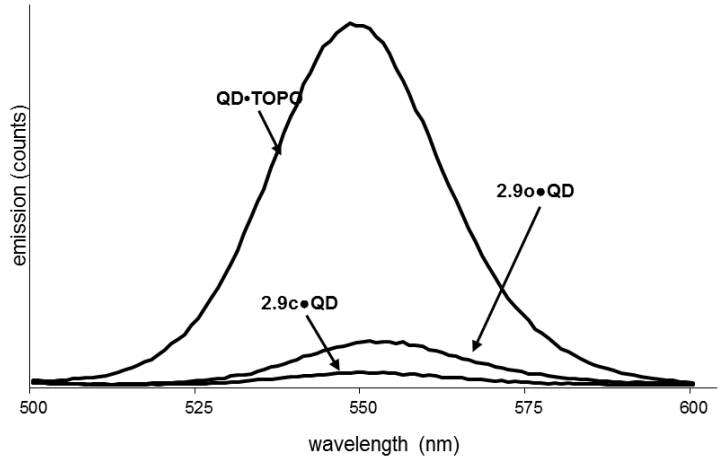

Figure 2.6 Emission spectra obtained from **QD•TOPO** and **2.9c•QD** in $CHCl_3$ solutions (1 x 10^{-6} M, 20° C, λ_{ex} = 490 nm). The spectrum labeled **2.9o•QD** was acquired from the solution containing **2.9c•QD** after irradiating it with >550 nm light for 150 s.

Cycling between the two species by alternately irradiating with UV and visible light allows toggling of luminescence intensity, but it also leads to a rapid decrease in the maximum emission intensity and an increase in the minimum, which are indicative of decomposition (Figure 2.7, inset). The QD absorption band centred at 530 nm remains unchanged during cycling attempts despite the increase in light scattering described above, implying degradation of the dithienylethene moiety rather than the QD. The comparatively small degree of decomposition observed while cycling between unbound dithienylethene isomers **2.9o** and **2.9c** suggests that degradation may be linked to the mechanism responsible for QD luminescence quenching.

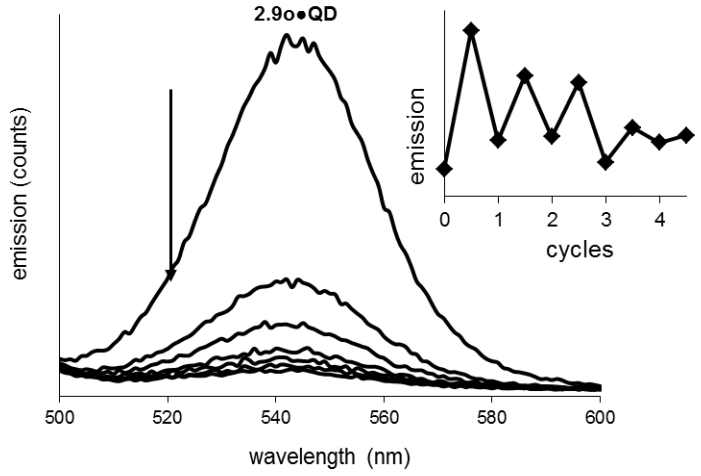

Figure 2.7 Emission spectra of **2.1o•QD** in $CHCl_3$ (1×10^{-6} M, 20° C, λ_{ex} = 490 nm) acquired during exposure to 313 nm light in 5 s intervals; arrows indicate the direction of spectral evolution during UV exposure. The inset depicts changes in emission of the same solution monitored at 550 nm during alternating periods of irradiation with UV (313 nm, 30 s) and visible light (>550 nm, 150 s).

2.3.4 Mechanistic Evaluation

The amount of luminescence quenching in **2.9o•QD** and **2.9c•QD** attributable to FRET can be estimated using Equation 2.1, which predicts the percentage of emitted light that is quenched by a suitable acceptor.

$$E = \frac{1}{1+(r/R_0)^6}$$

Equation 2.1 Expression for determining FRET efficiency *E*. *r* represents the centre-to-centre distance between donor and acceptor, and R_0 is the Förster radius of the pair.

A key parameter in this equation is the Förster radius R_0, which describes the centre-to-centre separation between donor and acceptor at which luminescence intensity is quenched to 50% of its unmodified value (Equation 2.2). Donor-acceptor pairs with $r > R_0$ exhibit quenching efficiencies less than 50%, whereas those with $r < R_0$ exhibit efficiencies greater than 50%. Systems in which the donor and acceptor are connected to one another by a flexible linker can have *r* values that vary dynamically (*e.g.* the biotin-streptavidin linker shown in Scheme 2.3); in such cases, the measured FRET efficiency reflects the average centre-to-centre distance between donor and acceptor.[20]

$$R_0^{\,6} = \frac{9000 Q_0 (\ln 10) \kappa^2 J}{128 \pi^5 n^4 N_A}$$

Equation 2.2 Expression for the Förster radius R_0 (nm). Q_o is the quantum yield of donor luminescence in the absence of quenching, κ is the transition dipole orientation factor, *J* is the spectral overlap integral, *n* is the refractive index of the solvent, and N_A is Avogadro's Number.

Evaluation of R_0 requires knowledge of two parameters peculiar to the donor-acceptor pair: the dipole orientation factor κ^2 and the spectral overlap integral *J*.[20]

The first quantity, κ^2, depends on the angle between the transition dipoles corresponding to donor emission and acceptor absorption, with theoretical values ranging from 0 – 4 (*i.e.* a value of 0 corresponds to perpendicular transition dipoles, and a value of 4 corresponds to parallel dipoles). Orientation factors can be approximated experimentally based on emission anisotropy measurements performed on both the donor and acceptor (*i.e.* thus requiring an acceptor moiety that emits light), but κ^2 is more commonly assigned a value of 2/3 based on the assumption that both donor and acceptor undergoing unrestricted isotopic motion.[20,43]

The second parameter, *J*, quantifies spectral overlap between the emission band of donor **QD•TOPO** and the absorption bands of its acceptor, **2.9o** or **2.9c**, prior to complex formation (Equation 2.3).[20]

$$J = \int \varepsilon_A(\lambda) F_D(\lambda) \lambda^4 d\lambda$$

Equation 2.3 Expression for the spectral donor-acceptor overlap integral *J* ($cm^3\ M^{-1}$). $\varepsilon_A(\lambda)$ is the molar extinction coefficient for light absorption by the acceptor (in $M^{-1}\ cm^{-1}$) and $F_D(\lambda)$ is the normalized luminescence intensity of the donor, both evaluated at wavelength λ (nm).

The spectral data depicted in Figure 2.8 thus enabled calculation of approximate *J* values for **QD•TOPO** and **2.9o** ($1.07 \times 10^{13}\ cm^3\ M^{-1}$), as well as for **QD•TOPO** and **2.9c** ($4.20 \times 10^{14}\ cm^3\ M^{-1}$). Using an assigned value of 2/3 for κ^2 (*i.e.* whose validity in this system is debatable due to restricted rotational freedom in the case of the quencher), the *J* values were then used to calculate R_0 for both donor-acceptor pairs: 18 Å for the former and 33 Å for the latter. Used in conjunction with the actual donor-acceptor separations in both complexes (*i.e.* approxi-

mately 37 Å, estimated based on the dimensions of the QD shown in Scheme 2.10 and structural models of compounds **2.9o** and **2.9c** constructed using Merck Molecular Force Field 94)[44] the R_0 values obtained provide theoretical FRET efficiencies of 1.3% and 33% for **2.9o•QD** and **2.9c•QD**, respectively, which indicate that differences in the projected FRET efficiencies may be at least partially responsible for differences in the amounts of luminescence quenching observed in the switch-QD complexes.

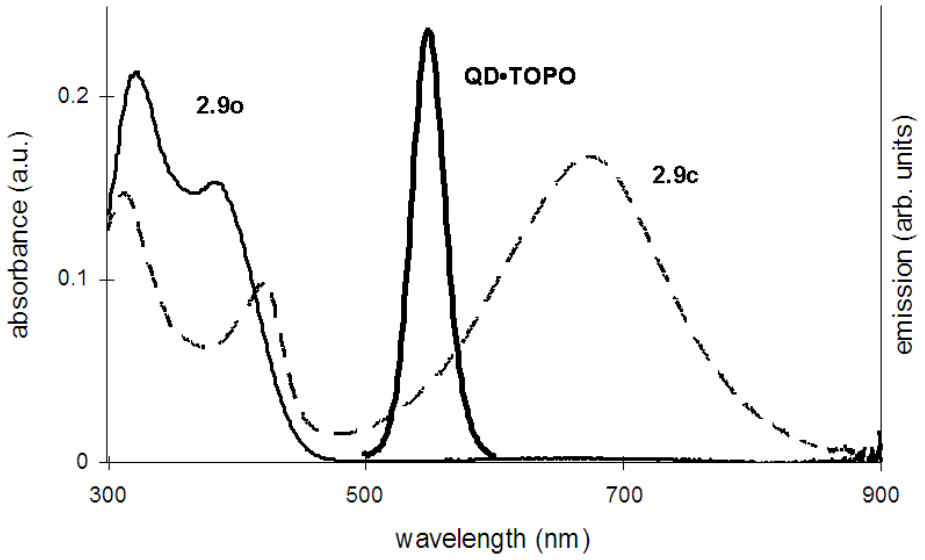

Figure 2.8 UV-vis absorbance spectra of **2.9o** (solid line) and **2.9c** (dashed line) in $CHCl_3$ (1×10^{-5} M, 20° C) juxtaposed with the emission spectrum of **QD•TOPO** (bold line) in $CHCl_3$ (1×10^{-6} M, 20° C, λ_{ex} = 490 nm). Spectral overlap integrals for **2.9o** and **2.9c** with **QD•TOPO** are approximately 1.07×10^{13} and 4.20×10^{14} cm^3 M^{-1}, respectively.

However, these calculations cannot rule out the possibility of luminescence quenching *via* a second, competing mechanism. Whether photoinduced electron transfer is plausible in complexes **2.9o•QD** and **2.9c•QD** as an added

source of luminescence quenching can be qualitatively assessed in terms of the activation barriers for those processes (Equation 2.4).[45]

$$\Delta G^{\ddagger}_{ET} = \frac{(\lambda + \Delta G^{\circ}_{ET})^2}{4\lambda}$$

Equation 2.4 Electron transfer activation energy $\Delta G^{\ddagger}_{ET}$. λ represents the reorganizational energy and ΔG°_{ET} the change in standard free energy accompanying electron transfer

Marcus theory asserts that the activation barrier for electron transfer exhibits a quadratic dependence on the sum of two terms: the energy λ associated with reorganization of the surroundings, and the electron transfer free energy ΔG°_{ET}. This suggests that increasing exergonicity lowers the activation barrier for electron transfer and accelerates the reaction; however, for reactions in which $\Delta G^{\circ}_{ET} < -\lambda$ (*i.e.* an energy regime referred to as the Marcus inverted region), increasing exergonicity leads to higher activation barriers. ΔG°_{ET} can be calculated using Equation 2.5.[46]

$$\Delta G^{\circ}_{ET} = e[E^{\circ}(D^{\bullet+}/D) - E^{\circ}(A/A^{\bullet-})] - \frac{e^2}{4\pi\varepsilon_0 e_r a} - \Delta E_{0,0}$$

Equation 2.5 The change in standard Gibbs Free Energy ΔG°_{ET} accompanying photoinduced electron transfer: e is the elementary charge, $E^{\circ}(D^{\bullet+}/D)$ is the reduction potential of the donor radical cation, $E^{\circ}(A/A^{\bullet-})$ is the reduction potential of the acceptor, ε_0 is the vacuum permittivity, e_r is the dielectric constant of the medium, a is the centre-to-centre separation between donor and acceptor, and $\Delta E_{0,0}$ is the emission energy of the donor.

The reduction potentials of acceptor compounds **2.9o** and **2.9c**, as well as the oxidation potential[47] and wavelength of maximum light emission by donor **QD•TOPO**, thus enabled calculation of the free energy changes ΔG°_{ET} accompa-

nying photoinduced electron transfer (Table 2.2). Electron transfer from **QD•TOPO** to ring-open dithienylethene **2.9o** is slightly endergonic, with $\Delta G°_{ET}$ equal to +0.57 meV. However, the anodic shift in acceptor reduction potential arising from photochemical conversion to the ring-closed isomer **2.9c** results in an exergonic reaction, with $\Delta G°_{ET}$ = -320 meV. Values of λ for analogous systems (*i.e.* in which there is a semiconductor-liquid interface) are commonly on the order of 400 – 500 meV,[48] suggesting that electron transfer in **2.9c•QD** probably occurs outside the Marcus-inverted regime and is much faster than in **2.9o•QD**, consistent with the data shown in Figure 2.6.

Table 2.2 Redox potentials and estimated changes in free energy accompanying electron transfer from **QD•TOPO** to compounds **2.9o** and **2.9c.**

	E_{ox}[a] / V	E_{red}[b] / V	$\Delta G°_{ET}$[c] / meV
QD•TOPO	+1.4[d]	—	—
2.9o	—	$-0.83_{(irr)}$[e]	+0.57
2.9c[f]	—	$-0.51_{(irr)}$[e]	-320

[a] First oxidation potential relative to SCE. [b] First reduction potential relative to SCE; the subscript *irr* indicates irreversibility. [c] Free energy changes corresponding to photoinduced electron transfer from donor **QD•TOPO** to acceptors **2.9o** or **2.9c**, calculated according to Equation 2.5 using an estimated donor-acceptor separation of 3.5 nm and emission wavelength of 550 nm. [d] Ref. 40. [e] Values referenced against an internal Fc/Fc^+ standard. [f] Generated by irradiating the solution of **2.9o** with 313 nm light until no further changes in the absorbance spectrum were observed.

2.4 **Conclusion**

2.4.1 Summary

A quencher-lumophore complex was successfully synthesized whose luminescence can be controlled using optical inputs. The complex features several variations on an existing design motif, utilizing the changes in optical and redox properties accompanying isomerization of a photoresponsive ligand to regulate the emission of light from an attached lumophore, in this case a quantum dot. Although this is not the first example in which a dithienylethene is employed rather than a spiropyran as the switching component, the dithienylethene architecture used in this system has the advantage of facile, direct coordination to the QD surface, as well as light absorption and redox properties attuned to luminescence quenching *via* electron transfer as opposed to FRET. These characteristics avoid the added synthetic complexity required for attachment of the dithienylethene to the QD *via* an intervening ligand and, in principle, the possibility of gradual quencher deactivation resulting from excited states generated by FRET.

QD luminescence is decreased to just 4% of its initial value following attachment of the ring-closed dithienylethene **2.9c**; photochemical conversion of the attached dye to its corresponding ring-open isomer **2.9o** results in a threefold restoration of the emitted light intensity. FRET efficiencies of 1.3% and 33% were calculated for complexes **2.9o•QD** and **2.9c•QD**, respectively, based on donor-acceptor spectral overlap measurements performed on the separate dithienylethene and QD components; these values account for only a small fraction of the drop in emitted light intensities observed in both complexes, suggesting addi-

tional luminescence quenching *via* a second mechanism. The barriers of activation for photoinduced electron transfer from **QD•TOPO** to **2.9o** and **2.9c** were examined qualitatively based on changes in free energy calculated using electrochemical data from each component. Photoinduced electron transfer in **2.9o•QD** is shown to be mildly endergonic; in **2.9c•QD**, however, electron transfer is strongly exergonic and likely outside the Marcus inverted regime. These observations suggest that electron transfer is plausible in both systems, but it is much more rapid in the latter.

A major limitation of the QD-dithienylethene complex is its susceptibility to photochemical degradation, which leads to a decrease in light emission from **2.9o•QD** and an increase in emission from **2.9c•QD** after only three cycles of alternating periods of irradiation with UV and visible light. Cyclic voltammetry experiments indicate that reduction of both dithienylethene isomers is electrochemically irreversible on the measurement timescales, suggesting possible decomposition of the dye following photoinduced electron transfer from the QD; this is supported by the observation that repeated photoisomerization of the unbound dithienylethene leads to comparatively little decomposition.

2.4.2 Prospective Research

Future research should focus initially on providing a more thorough understanding of the mechanisms responsible for luminescence quenching and photochemical decomposition of the dithienylethene-QD complex. Transient absorption spectroscopy would assist in both regards by making it possible to identify and monitor short-lived species formed immediately after radiationless deactivation of

the QD. Additional insight into the degradative process would be provided by structural analysis of the chemical products generated from the neutral dithienylethene radical, which would likely require preparative-scale electrolyses of unbound dithienylethenes **2.9o** and **2.9c**. Depending on the results of these experiments it might be possible to design a modified dithienylethene ligand in which the likelihood of degradation following electron transfer from an excited QD would be minimized without compromising the ability of the system to reversibly control light emission (*e.g.* if degradation proceeds *via* the routes shown in Schemes 1.2 and 1.3, a more stable molecular switch design might replace the thiophene units in compounds **2.9o** and **2.9c** with benzothiophenes; however, this could also result in different luminescence quenching efficiencies from those described in this chapter).

2.5 **Experimental**

2.5.1 Materials

All solvents used for synthesis, electrochemistry, UV-vis absorption spectroscopy and fluorimetry were purchased from Aldrich or Fisher and, except for THF and Et_2O, used without further purification. THF and Et_2O were dried over sodium metal and distilled under N_2. Solvents for NMR spectroscopy were purchased from Cambridge Isotope Laboratories and used as received. Reagents and starting materials were purchased from Aldrich and, except for Bu_4NPF_6 and ferrocene, used without further purification. Bu_4NPF_6 was recrystallized 3 times from EtOH and dried *in vacuo* at 110° C for 3 days, then stored in a desiccator. Ferrocene was purified by sublimation and also stored in a desiccator until need-

ed. Compounds **2.7** and **2.8** were prepared according to literature procedures.[37,38] TOPO-decorated, CdSe-ZnS core-shell quantum dots (**QD•TOPO**) were provided courtesy of Professor Françisco M. Raymo (University of Miami, Department of Chemistry). Column chromatography was performed using 230-400 mesh silica gel 60 purchased from Silicycle, Inc., or 80-200 mesh neutral alumina purchased from Fisher.

2.5.2 Instrumentation

NMR spectroscopy was performed on a Bruker Avance 600 MHz NMR spectrometer. ^{1}H NMR spectra were acquired using an equipped TCI cryoprobe and ^{13}C NMR spectra were acquired using a QNP cryoprobe. Chemical shifts are reported in parts per million relative to TMS using the residual solvent peak as a reference standard. Coupling constants are reported in hertz. UV-vis absorbance measurements were performed using a Varian Cary 300 Bio Spectrometer. Fluorescence measurements were carried out on chloroform solutions ($1x10^{-6}$ M) in 10 mm quartz cuvettes using a Photon Technology International QuantaMaster spectrometer with the excitation wavelength set to 490 nm. Mass spectrometry measurements were performed using a Varian 4000 GC/MS operating at an ionization energy of 70 eV. Cyclic voltammetry measurements were carried out using a Pine AFCBP1 bipotentiostat.

2.5.3 Photochemistry

Ring-closing reactions were carried out with 313 nm light from a handheld UV lamp (Spectroline E-Series, 3.5 mW cm^{-2}). Ring-opening reactions were per-

formed using light from a 300 W tungsten source passed through a 550 nm cutoff filter. Photoreactions monitored by UV-vis spectroscopy were performed on 10 μM $CHCl_3$ solutions in 1 cm quartz cuvettes and typically required 150 s and 30 s for ring-opening and ring-closing reactions to reach their respective photostationary states.

2.5.4 Electrochemistry

Cyclic voltammetry measurements were performed on samples dissolved in CH_3CN (1.0 mM) using a cell consisting of a polished platinum working electrode, a platinum coil counter electrode, a Ag wire reference electrode and 0.1 M Bu_4NPF_6 as the supporting electrolyte. All voltammograms were acquired using scan rates between 100-300 mV s^{-1} and all peak potentials referenced to a ferrocene internal standard (+475 mV *vs.* SCE). The platinum working electrode was cleaned before each experiment by polishing over 5 μm and then 1 μm diamond paste, followed by sonication in distilled water for 2 min. The electrode was then rinsed with ethanol and air dried.

2.5.5 Synthesis

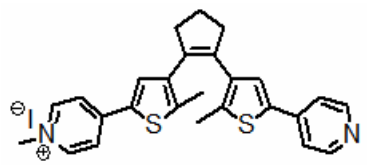

2.9o

Synthesis of compound (2.9o)

A solution of MeI (6 µL, 0.1 mmol) in CH_2Cl_2 (10 mL) was added dropwise over 10-15 min to a stirring solution of compound **2.8** (0.040 g, 0.10 mmol) in CH_2Cl_2 (15 mL) under N_2, after which the reaction mixture had become pale yellow. After stirring for 16 h at room temperature, the reaction mixture was washed 3 times with distilled water and the combined organic layers adsorbed onto neutral alumina (Grade II-III). The compound was purified by flash column chromatography with 5% MeOH in CH_2Cl_2 containing 1 drop of Et_3N for every 20 mL of eluent. Fractions containing the second major band to elute were concentrated to dryness *in vacuo*, affording 26 mg (47%) of **2.9o** as a pale yellow solid.

^{1}H NMR (600 MHz, $CDCl_3$, *δ*): 9.25 (d, *J* = 6.6 Hz, 2H), 8.50 (d, *J* = 6.0 Hz, 2H), 7.87 (d, *J* = 7.2 Hz, 2H), 7.59 (s, 1H), 7.30 (d, *J* = 6.0 Hz, 2H), 7.15 (s, 1H), 4.56 (s, 3H), 2.83 (t, *J* = 7.2 Hz, 4H), 2.10 (p, *J* = 7.2 Hz, 2H), 2.05 (s, 3H), 1.99 (s, 3H). ^{13}C NMR (100 MHz, $CDCl_3$, *δ*): 150.43, 144.33, 141.59, 137.28, 135.02, 128.49, 126.49, 123.31, 120.31, 119.47, 119.45, 48.55, 38.67, 38.65, 29.90, 27.93. HRMS (ESI) *m/z* calculated for $C_{26}H_{25}N_2S_2$ (M-I$^-$) 429.1442, found 429.1459.

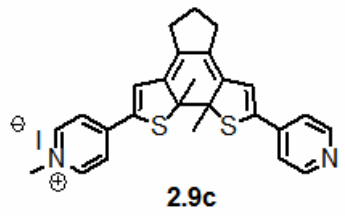

2.9c

Synthesis of compound (2.9c)

To a quartz NMR sample tube was added a solution of compound **2.9o** (6 mg, 10 µmol) in $CDCl_3$ (1 mL). The tube was capped and laid on its side, 1 cm

below a downward-facing, handheld UV lamp. The solution was irradiated with 313 nm light for 15 min, during which the reaction mixture was agitated by gently rolling the sample tube back and forth beneath the lamp. Analysis of the crude solution by ^{1}H NMR spectroscopy revealed a mixture consisting predominantly of the ring-closed isomer. Exposure of the solution to 313 nm light for another 5 min resulted in no further change in composition, indicating that the photostationary state had been reached (PSS_{313} = 93% compound **2.9c**). Concentration of the solution to dryness *in vacuo* afforded the mixture as a blue film (6 mg, 10 μmol), which was used without further purification.

^{1}H NMR (600 MHz, $CDCl_3$, δ): 9.21 (d, J = 6.0 Hz, 2H), 8.62 (d, J = 5.4 Hz, 2H), 7.90 (d, J = 6.6 Hz, 2H), 7.36 (d, J = 5.4 Hz, 2H), 7.21 (s, 1H), 6.60 (s, 1H), 4.63 (s, 3H), 2.65 (t, J = 7.2 Hz, 2H), 2.54 (t, J = 7.2 Hz, 2H), 2.03 (s, 3H), 2.02 (s, 3H), 1.97 (p, J = 7.2, 2H).

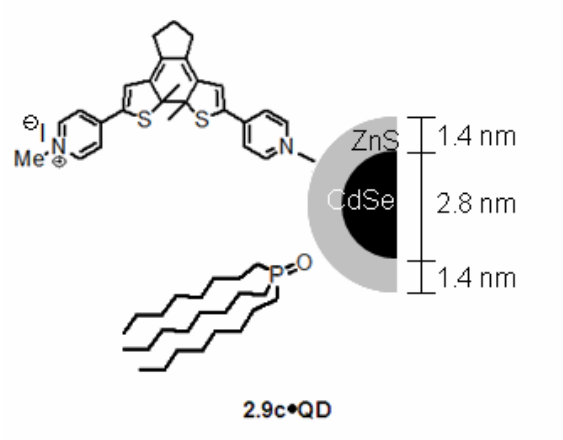

2.9c•QD

Synthesis of 2.9c•QD

To a solution of **QD•TOPO** (4 mg) in $CHCl_3$ (4 mL) was added crude compound **2.9c** (4 mg, 7 μmol). The mixture was then heated to reflux under N_2 while

stirring magnetically for 1 h, then allowed to cool to room temperature upon standing. CH_3CN (4 mL) was added, resulting in the formation of a turquoise precipitate. The suspension was centrifuged and the supernatant liquid decanted. The pellet was redissolved in fresh $CHCl_3$ (4 mL) and treated once more with CH_3CN (4 mL). After the suspension had been centrifuged and the supernatant decanted a second time, the dark blue sediment was redissolved in $CHCl_3$ (1 mL), affording a stock solution suitable for UV-vis spectroscopic and fluorimetric studies.

CHAPTER 3: CONTROLLING THERMORESPONSIVE MATERIALS WITH MOLECULAR SWITCHING

3.1 Thermoresponsive Systems

3.1.1 Introduction

Despite the superior specificity afforded by optical stimuli, changes in temperature are often more convenient for manipulating materials. From a design perspective, controlling the properties of a material by modifying its chemical composition is made relatively straightforward by the nearly ubiquitous dependence of chemical reaction rates on temperature (*i.e.* increasing the temperature of a reaction usually accelerates it, and decreasing its temperature usually slows it down). In contrast, eliciting similar changes in a material using optical stimuli is complicated by requirements that it absorb light efficiently at those wavelengths and that it undergo excited state deactivation *via* one pathway as opposed to another (*e.g.* isomerization *versus* luminescence, internal conversion, or proton transfer). From a practical perspective, heat diffusion in condensed phases yields a more even distribution of the stimulus than can be readily obtained using light, whose ability to penetrate materials is significantly limited by wavelength-dependent scattering.

3.1.2 Reversible Bond-Forming Reactions

The temperature dependence of chemical equilibria established by reversible bond-forming reactions makes them well-suited to the design of ther-

moresponsive systems. For instance, the assembly of a hypothetical compound **AB** and its dissociation into components **A** and **B** are competing processes that give rise to an equilibrium mixture whose composition varies as a function of temperature (Scheme 3.1). At temperature T_1, the equilibrium favours formation of compound **AB** (Scheme 3.1a), whereas substances **A** and **B** predominate at T_2 (Scheme 3.1b). In this manner the composition and properties of a material (or system of interacting materials) can be made to vary in response to changes in temperature.

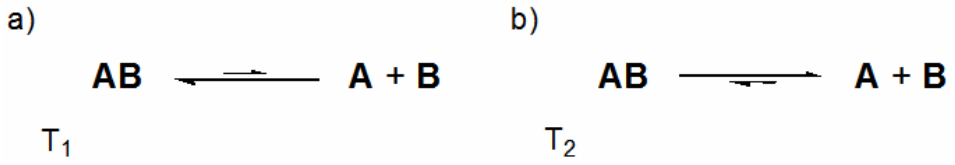

Scheme 3.1 Reversible dissociation of a compound **AB** into separate compounds **A** and **B** at different temperatures T_1 and T_2: (a) **AB** predominates at T_1, (b) whereas dissociation is favoured at T_2.

The Diels-Alder (DA) reaction between furan and maleimide is an apt example of such a reaction. At low to moderate temperatures (between 25° – 70° C) the reaction equilibrium favours the *endo* cycloaddition product (Scheme 3.2a), though raising the temperature to between 70° – 100° C leads to a gradual shift of the equilibrium composition to favour the *exo* adduct (Scheme 3.2b). Greater temperatures lead to an equilibrium mixture that consists predominantly of the free diene and dienophile (Scheme 3.2c).[49]

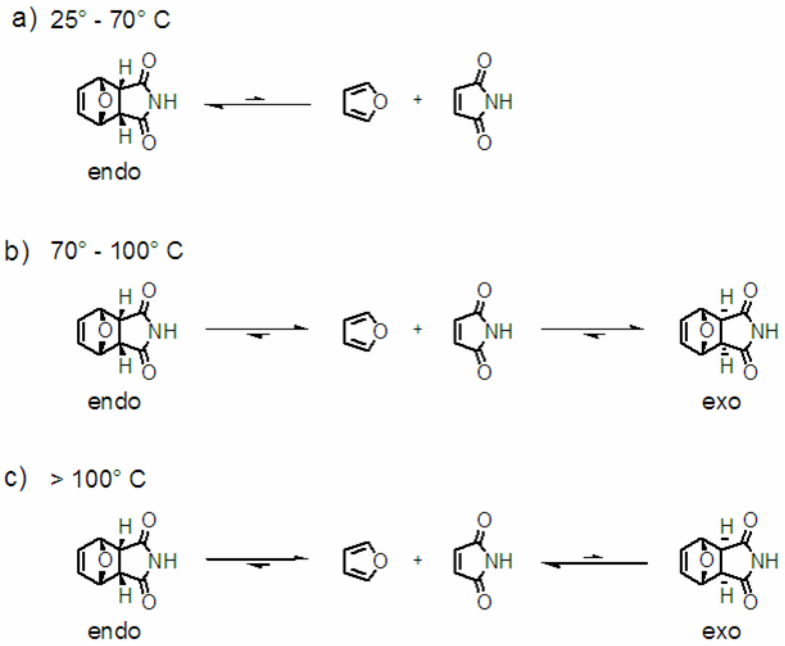

Scheme 3.2 The equilibrium composition of the DA reaction between furan and maleimide varies with temperature: (a) at temperatures between 25° – 70° C, the *endo* adduct is favoured; (b) the *exo* adduct predominates between 70° – 100° C; (c) at higher temperatures, the free diene and dienophile are more abundant than either adduct.

These features are consistent with qualitative observations concerning the potential energies of the various species involved in the DA reaction equilibrium as they vary with nuclear geometry along the reaction coordinate (Figure 3.1). At low to moderate temperatures, the combined energy of the free diene and dienophile is sufficient to overcome the activation barrier leading to formation of the *endo* adduct but not the *exo* (*i.e.* due to stabilizing interactions between orbitals on furan and maleimide that occur in the former transition state but not the latter).[50] The reaction is exothermic since it corresponds to formation of two low-energy sigma bonds at the expense of two high-energy pi bonds, and the resulting barrier to the reverse reaction leads to a much lower rate of cycloreversion *via* the retro-DA reaction in this temperature regime.

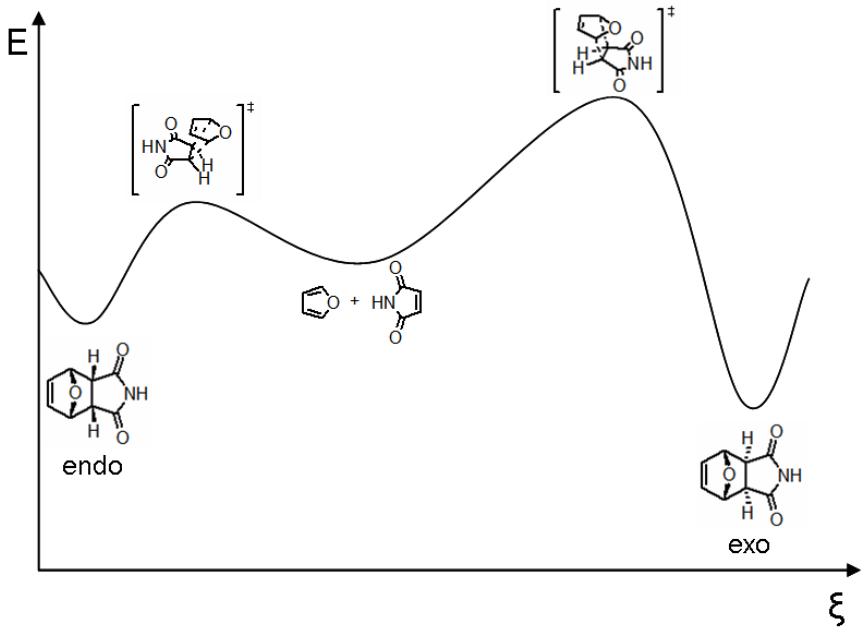

Figure 3.1 Qualitative potential energy surface corresponding to formation of *endo* and *exo* cycloaddition products from furan and maleimide *via* the DA reaction.

Higher temperatures provide the *endo* adduct with sufficient energy to proceed beyond the immediate cycloreversion barrier (regenerating furan and maleimide) as well as the activation barrier that leads to formation of the *exo* product. Isomerization in this manner is exothermic overall because of reduced steric congestion in the *exo* species relative to the *endo*, resulting in the barrier to cycloreversion from the *exo* compound being significantly greater than any other activation barrier along the reaction coordinate. Consequently, temperatures high enough to facilitate cycloreversion of the *exo* moiety lead to dynamic interconversion of species along all three minima. At such temperatures the equilibrium favours a product distribution that maximizes the entropy of the system. Furan and maleimide, together, have more degrees of freedom (and thus greater entropy) than either of the two cycloaddition products (reflected in the breadth of the bimo-

lecular potential energy well relative to the other two minima shown in Figure 3.1) and are thus the most abundant species under these conditions.

3.1.3 Technologies

The reversibility of the DA reaction and its sensitivity to temperature make it an attractive motif for technologies that benefit from covalent bonding at one set of conditions (low to moderate temperatures) and bond cleavage at another (high temperatures). For instance, the DA reaction between hydrophobic diene **3.1** and hydrophilic dienophile **3.2** yields adduct **3.3** (Scheme 3.3), whose amphiphilic character (*i.e.* arising from the hydrophobic dodecyl chain and hydrophilic carboxylate group) enables it to act as a surfactant and to form micelles in aqueous environments. At higher temperatures **3.3** undergoes cleavage into its respective hydrophobic and hydrophilic precursors, resulting in the loss of amphiphilic character and micellar collapse.[51] This is an extremely desirable feature among industrial surfactants for reasons both practical (*e.g.* in proteomics, removal of the surfactant following in-gel digestion protocols)[52] and environmental (*i.e.* lower concentrations of hazardous materials in waste water).[53,54,55]

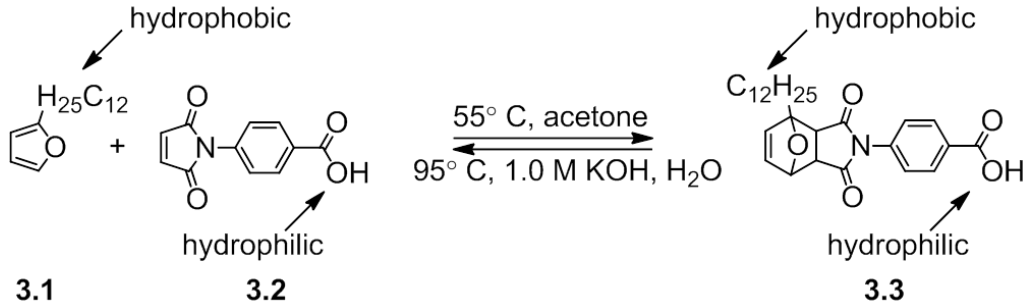

3.1 **3.2** **3.3**

Scheme 3.3 Amphiphilic surfactant **3.3** prepared by the DA reaction between hydrophobic **3.1** and hydrophilic **3.2**. Exposure of adduct **3.3** to higher temperatures results in loss of amphiphilic character due to cleavage *via* the retro-DA reaction.

DA chemistry also ameliorates a major shortcoming among covalent network polymers, whose great mechanical strength generally comes at a price: stress sufficient to damage the polymer results in cleavage of chemical bonds. Consequently, attempts to mend damage regions using physical methods (*i.e.* welding, glues or adhesives) are incapable of restoring the polymer to its original strength. However, in the case of covalent network polymers assembled using the DA reaction, bond cleavage due to mechanical stress is localized predominantly among DA adducts due to the relatively low activation barrier of the retro-DA reaction compared to cleavage of other bonds present in the polymer (Scheme 3.4). As a result, damaged regions can be reconstituted at the molecular level *via* the DA reaction between free dienes and dienophiles present in the polymer matrix.[56]

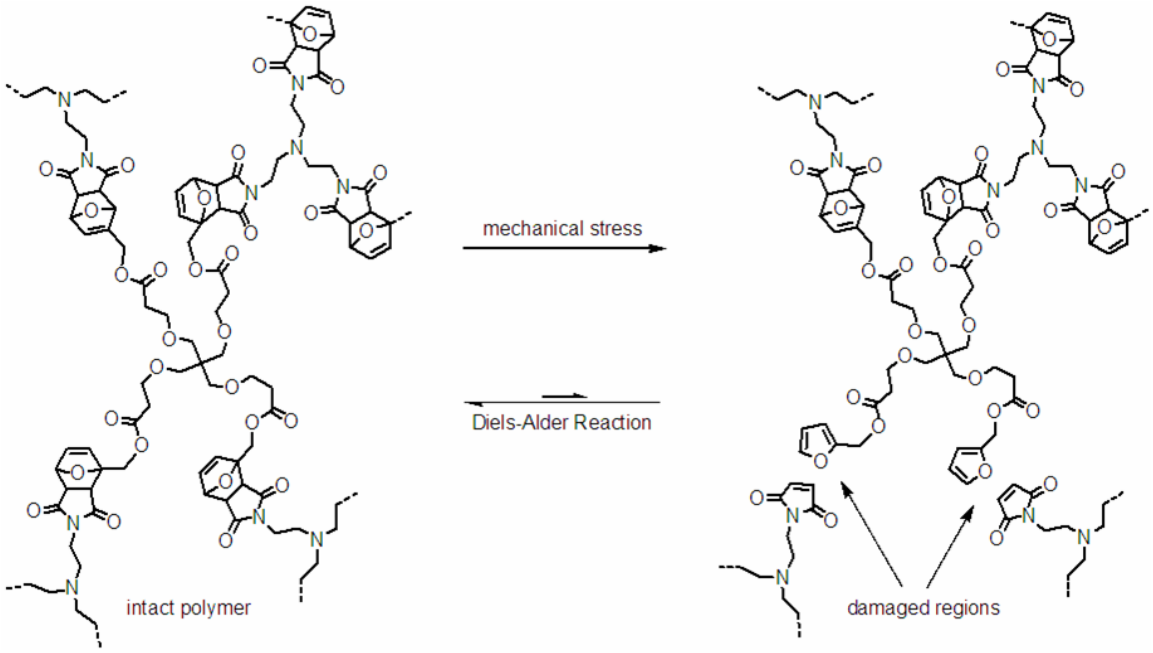

Scheme 3.4 The DA reaction between free dienes and dienophiles in a self-healing polymer spontaneously mends regions damaged by mechanical stress.

The DA reaction is an attractive candidate for dynamic combinatorial chemistry due to its ability to reversibly generate multiple three-dimensional architectures from a single pair of planar reactants. The dienes and dienophiles shown in Scheme 3.5 undergo rapid cycloaddition and cycloreversion at room temperature, resulting in a dynamic library of twelve adducts at various concentrations.[57] Such mixtures can be screened directly and in real time for qualities like protein binding affinity, which causes the reaction equilibrium to favour formation of a substance being bound. The bound molecule can then be identified and evaluated as a possible pharmaceutical lead.[58,59]

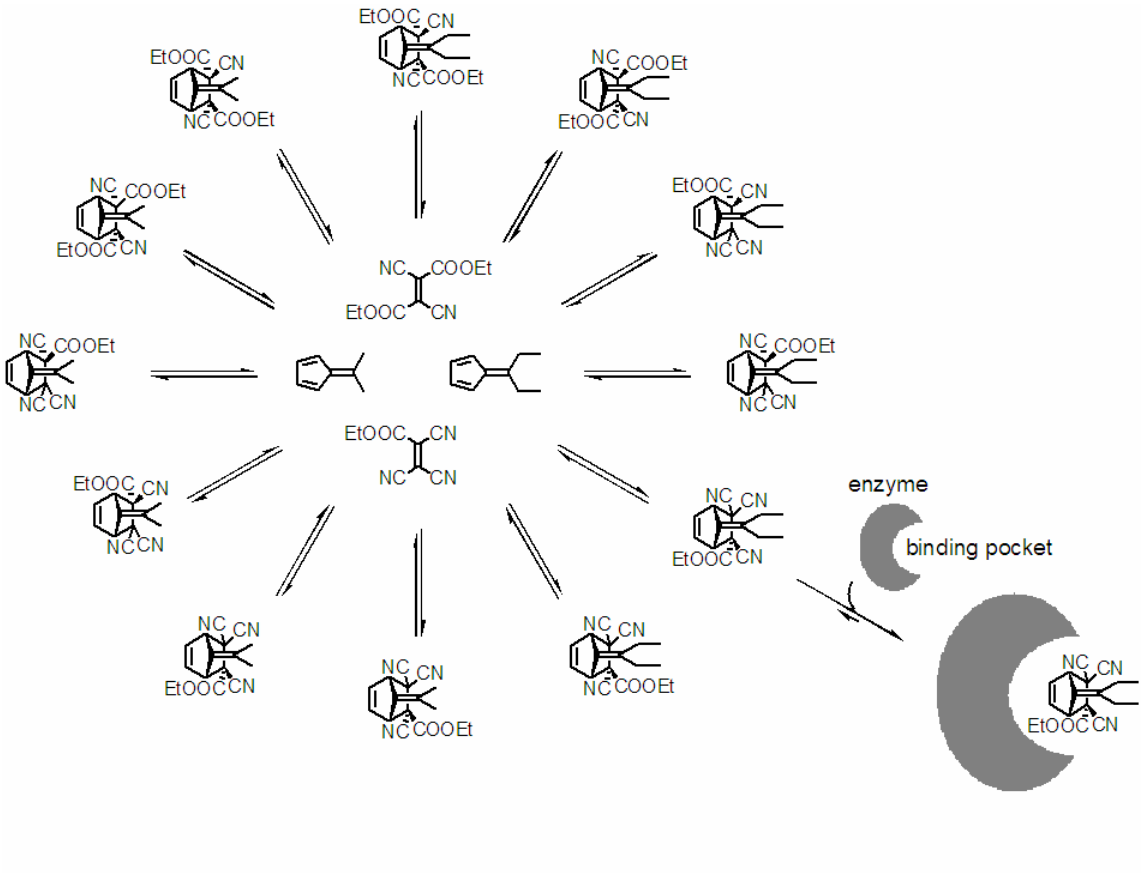

Scheme 3.5 A dynamic combinatorial library of twelve compounds generated *via* DA reactions between one of two dienes and one of two dienophiles, screened on the basis of protein binding affinity.

3.2 Controlling the Reversibility of Bond Formation

3.2.1 Incentive

The potential usefulness of technologies based on thermoresponsive systems is mitigated by effects arising from circumstantial exposure to temperatures outside the desired regime, which can be difficult to avoid in many working environments. In the case of cleavable surfactants, this can cause premature thermolysis (*i.e.* prior to emulsification) and render them incapable of micelle formation, whereas self-healing polymers like the one shown in Scheme 3.4 under-

go a loss of mechanical strength and integrity. Similarly, changes in temperature can cause compounds isolated from dynamic combinatorial libraries to spontaneously regenerate the mixtures from which they were isolated.

3.2.2 Photoresponsive DA Adducts

These limitations can be circumvented by harnessing a second set of stimuli to selectively toggle the reversibility of the bond-forming reaction, allowing it to be turned “off” when bond cleavage is undesirable (*e.g.* during isolation and identification of compounds obtained from dynamic combinatorial libraries) and turned back “on” when it is beneficial (*e.g.* to facilitate the collapse of micelles formed from cleavable surfactants). In general, a pair of compounds **A** and **B** that reversibly react to form **AB** at a temperature T_1 can be tailored such that **AB**, when exposed to an appropriate set of conditions designated “off”, is transformed irreversibly into compound **CD** (Scheme 3.6a). Consequently, **CD** remains intact at temperatures T_2 that would otherwise cause **AB** to dissociate into its precursor compounds (Scheme 3.6b). Depending on the nature of the reaction that forms **CD**, it may be possible to regenerate compound **AB** *via* another set of conditions, “on”, permitting dissociation into **A** and **B** (Scheme 3.6c).

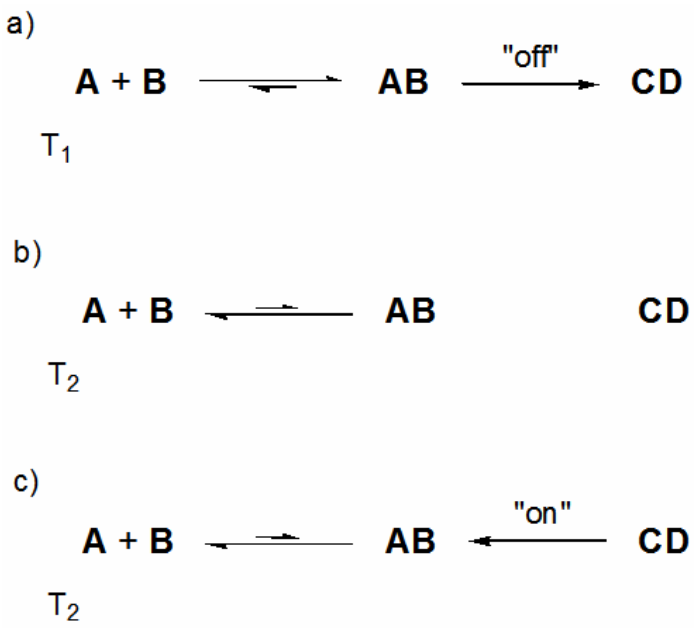

Scheme 3.6 (a) At temperature T_1, compounds **A** and **B** reversibly form compound **AB**, which can be made to irreversibly form compound **CD** when exposed to a set of conditions designated “off”. (b) At T_2, **AB** dissociates into **A** and **B**, but **CD** remains intact. (c) A different set of conditions, “on”, turns **CD** back into **AB**, which readily dissociates into **A** and **B** at T_2.

The veracity of this approach is illustrated by the DA reaction between dithienylfulvene **3.4** and diethyldicyanofumarate (Scheme 3.7). The resulting adduct **3.5o** contains a *cis*-hexatriene motif, enabling conversion of **3.5o** to its corresponding ring-closed isomer **3.5c** upon exposure to UV light (313 nm). The former isomer is capable of thermolysis *via* the retro-DA reaction at room temperature, whereas the latter is not. Presumably, this is because ring-closure results in loss of the carbon-carbon double bond connecting the two thiophenes in **3.5o**, which is a necessary prerequisite for the retro-DA reaction. Consequently, the ring-closing reaction effectively negates the reversibility of the DA reaction, and the ring-opening reaction (*i.e.* resulting from irradiation of **3.5c** with visible

light having wavelengths >434 nm), by regenerating **3.5o**, effectively restores the reversibility of the DA reaction.[60]

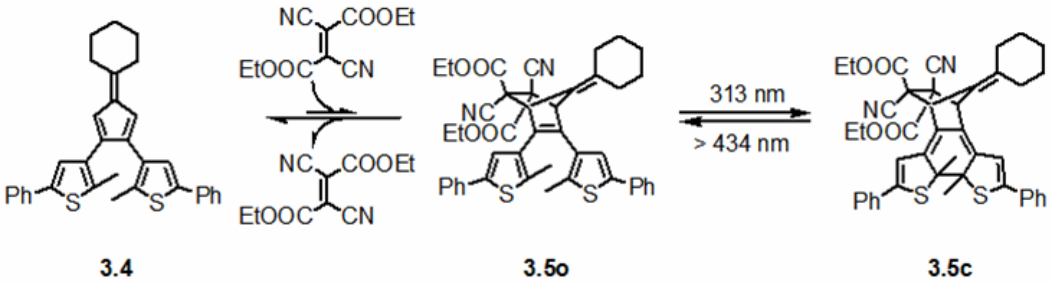

Scheme 3.7 The reversible DA reaction between dithienylfulvene **3.4** and diethyldicyanofumarate, photochemically gated by interconversion of adduct **3.5o** with its corresponding ring-closed isomer **3.5c** using UV (313 nm) and visible light (>434 nm). The former spontaneously undergoes cleavage *via* the retro-DA reaction at room temperature, whereas the latter does not.

In this system, the DA reaction equilibrium favours dissociation of **3.5o** into fulvene **3.4** and the cyanoolefin at room temperature, a feature that makes it attractive for applications that benefit from spontaneous cleavage upon irradiation with visible light (*e.g.* targeted drug delivery) and technologies in which higher temperatures may be detrimental (*e.g.* during screening of dynamic combinatorial libraries). Other applications, however, require systems in which the DA adduct predominates at room temperature (*e.g.* self-healing polymers and cleavable surfactants). Such disparate technological demands expose the need for molecular switches capable of regulating DA reaction equilibria spanning a range of temperatures.

Molecular switches with these traits can be designed, in principle, by varying the diene and the dienophile, whose structural features determine whether a particular DA reaction equilibrium favours adduct formation or thermolysis at a

given temperature by adjusting the activation energies of the two processes relative to one another. Indeed, the fact that dissociation of compound **3.5o** predominates at room temperature is consistent with the behavior of DA adducts prepared from fulvenes[61] and cyanoolefins,[62] both of which lower the retro-DA activation barrier relative to adducts prepared from furan[63] and maleimide.[41] This suggests that ring-open molecular switches based on adducts of dithienylfuran and maleimide might persist at room temperature, undergoing thermolysis *via* the retro-DA reaction upon heating to temperatures greater than 100° C. Similarly, ring-open switches synthesized from dithienylfuran and cyanoolefins might undergo thermolysis at intermediate temperatures.

To test these hypotheses, dithienylfuran compounds **3.6a-c** were synthesized and screened based on their abilities to form DA adducts with different dienophiles (Scheme 3.8). The dienophiles employed in these studies afford a range of reactivities as a result of varying electron deficiencies (*i.e. N*-ethylmaleimide being the least reactive of the three, tetracyanoethylene being the most reactive, and diethyl dicyanofumarate being intermediate between the two) and were selected in order to adjust the temperatures at which adduct formation and thermolysis might take place. Different substituents present on **3.6a-c** (*i.e.* phenyl, chloro, and ester substituents) were selected on a similar basis to further tune the DA reaction equilibria. Each of the DA adducts was then examined with respect to its ability to undergo the photochemical ring-closing and ring-opening reactions typical of dithienylethenes. Adducts amenable to photoisomerization

were further probed in order to ascertain the effects of photoswitching on the retro-DA reaction.

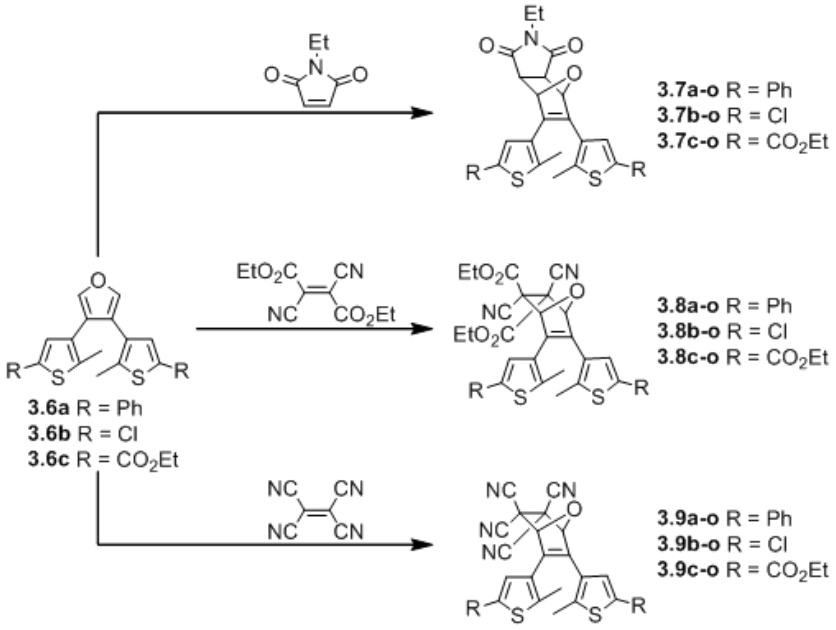

Scheme 3.8 Screening of dithienylfuran compounds **3.6a-c** based on DA adduct formation with different dienophiles.

3.3 **Results and Discussion**

3.3.1 Synthesis

Dithienylfuran compounds **3.6a-c** were ultimately synthesized using a two-fold Suzuki reaction carried out between dibromofuran and thiopheneboronic acid cross-coupling partners. The former compound **3.10** was prepared in modest yield *via* oxidative cyclodehydration of (*E*)-2,3-dibromo-2-butene-1,4-diol in aqueous chromic acid following a literature procedure (Scheme 3.9a).[64] The latter compounds were prepared from bromothiophenes **3.12a-b**, both of which were synthesized by different routes from 2-methylthiophene (Scheme 3.9b). Dibromination of 2-methylthiophene under acidic conditions yielded 2,4-dibromo-5-

methylthiophene **3.11**,[65] which then underwent Suzuki coupling with phenyl-boronic acid to afford compound **3.12a**.[66] Chlorination of 2-methylthiophene with NCS yielded 2-chloro-5-methylthiophene, which was then treated with bromine to furnish compound **3.12b**.[36]

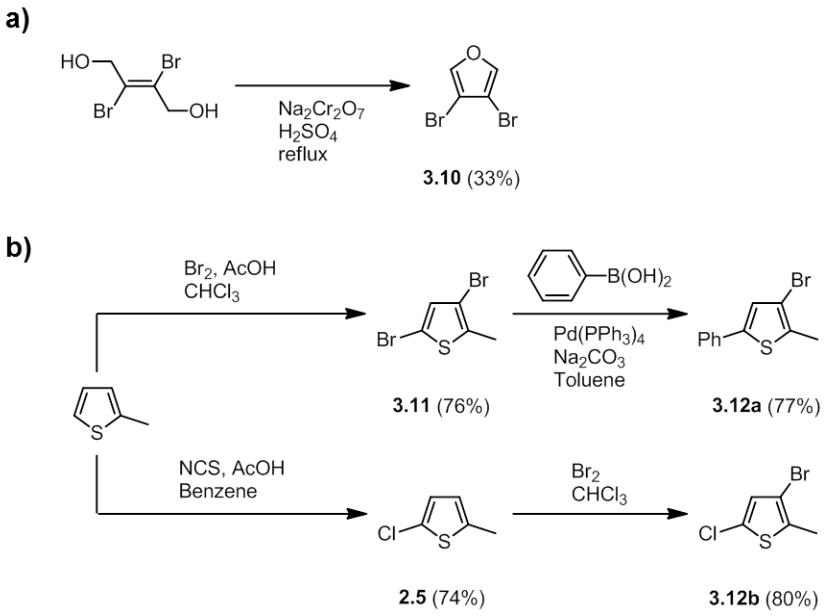

Scheme 3.9 Synthesis of (a) dibromofuran **3.10** and (b) bromothiophenes **3.12a** and **3.12b**.

Bromothiophenes **3.12a-b** were converted to their corresponding boronic acid derivatives in a one-pot procedure *via* lithium-halogen exchange, followed by boronylation with tris-(*n*-butyl)borate and acid-catalyzed hydrolysis of the resulting boronate ester (Scheme 3.10).[67] Twofold Suzuki cross-coupling of boronic acids **3.13a-b** with 3,4-dibromofuran **3.10** afforded symmetrical dithienylfuran compounds **3.6a-b** in modest yields in addition to products resulting from reductive dehalogenation of the mono-coupled intermediates.[68] A third dithienylfuran compound bearing ester substituents was synthesized from compound **3.6b** by

lithium-halogen exchange, carboxylation with gaseous CO_2, and then acidification of the carboxylate salt and Fischer esterification in ethanol.

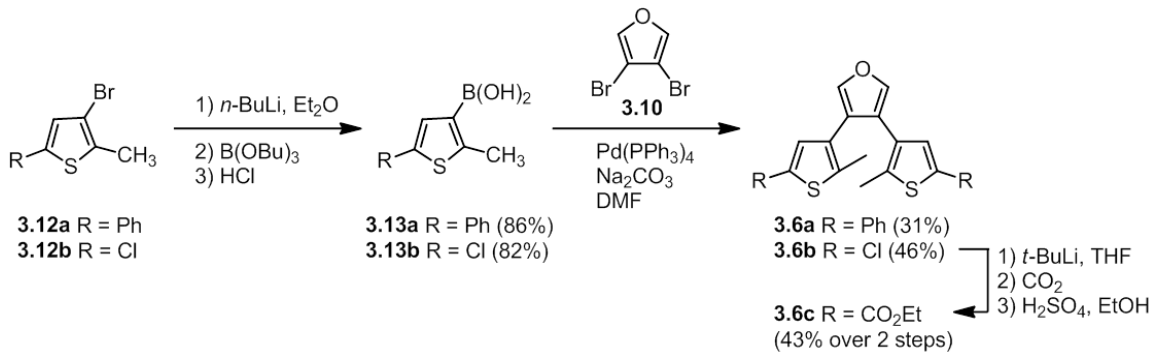

Scheme 3.10 Synthesis of dithienylfuran compounds **3.6a-c**.

3.3.2 DA Reaction Screening

Each of the dithienylfuran compounds **3.6a-c** was screened based on its ability to form DA adducts with different dienophiles, beginning with *N*-ethylmaleimide (Table 3.1). The reactions were carried out in deuterated solvents in order to track their progress by ^{1}H NMR spectroscopy. Dithienylfuran compounds bearing chloride or ester substituents (*i.e.* compounds **3.6b** and **3.6c**, respectively) both formed adducts in the presence of equimolar concentrations of *N*-ethylmaleimide when heated at 70° C. Each of the two adducts was found to consist exclusively of the *exo* isomer based on the lack of observable nuclear spin-coupling between protons at the maleimide and furan bridgehead positions.[69] However, no reaction was observed under these conditions in the case of the diphenyl derivative **3.6a**. Subsequent attempts to form adduct **3.7a-o** were carried out at higher reaction temperatures (*i.e.* in order to compensate for the possibility of a heightened activation barrier relative to adducts formed from the

dichloro and diester derivatives) and at room temperature using an excess of the dienophile (*i.e.* to address the possibility of slow adduct formation at low-to-moderate temperatures followed by thermolysis upon heating to 70° C), but these attempts were also unsuccessful.

Table 3.1 Screening of dithienylfuran compounds for DA adduct formation with *N*-ethylmaleimide

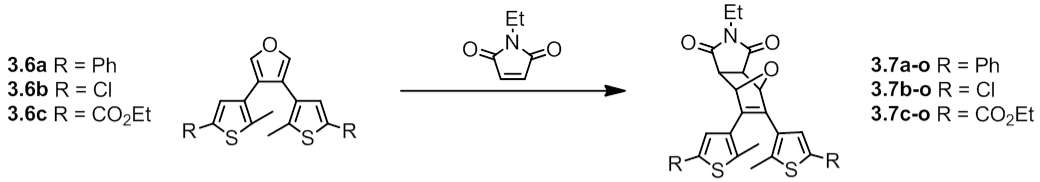

diene	*stoichiometry*[a]	*solvent*	*temperature / °C*	*time / h*	*product*	*yield / %*
3.6a	1:1	$CDCl_3$	70	24	**3.7a-o**	0[b]
3.6a	1:1	DMSO-d_6	80	24	**3.7a-o**	0[b]
3.6a	1:1	DMSO-d_6	90	24	**3.7a-o**	0[b]
3.6a	1:3	DMSO-d_6	21	138	**3.7a-o**	0[b]
3.6b	1:1	$CDCl_3$	70	24	**3.7b-o**	79[c]
3.6c	1:1	$CDCl_3$	70	38	**3.7c-o**	65[c]

[a] Expressed as the molar ratio of diene to dienophile. [b] Yields determined by ^{1}H NMR spectroscopy. [c] Isolated yields.

Dithienylfuran compounds **3.6a** and **3.6c** were then screened for the ability to form DA adducts with diethyl dicyanofumarate (Table 3.2). Further exploration of adducts based on the dichloro derivative **3.6b** were abandoned (*i.e.* due to the poor photochemical stability of compound **3.7b-o**, discussed later). Solutions containing the diphenyl derivative **3.6a** developed an intense red colour immediately upon mixing with diethyl dicyanofumarate (Figure 3.2). However, ^{1}H NMR

spectra acquired from the mixtures were indistinguishable from spectra obtained from the separate starting materials, suggesting that the red colour that had developed upon mixing was due to formation of a charge transfer complex as opposed to the desired DA adduct **3.8a-o**. No reaction was observed in the case of the diester compound **3.6c**, either. This came as a surprise, given the heightened reactivity towards dienophiles generally exhibited by diethyl dicyanofumarate relative to *N*-ethylmaleimide, which had successfully undergone the DA reaction with diester compound **3.6c** to form adduct **3.7c-o**. Subsequent attempts to elicit adduct formation by varying the reaction temperatures and reagent stoichiometries were similarly unsuccessful.

Table 3.2 Screening of dithienylfuran compounds for DA adduct formation diethyl dicyanofumarate.

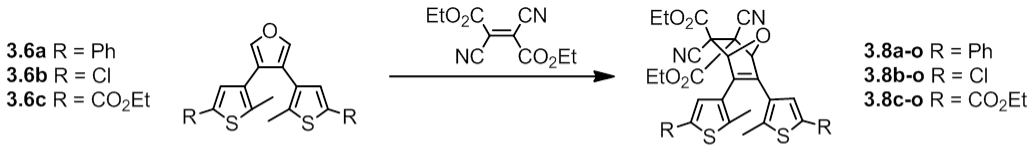

diene	*stoichiometry*[a]	*solvent*	*temperature / °C*	*time / h*	*product*	*yield / %*
3.6a	1:1	$CDCl_3$	21	24	**3.8a-o**	0[b]
3.6c	1:1	$CDCl_3$	70	24	**3.8c-o**	0[b]
3.6c	1:1	$CDCl_3$	40	24	**3.8c-o**	0[b]
3.6c	1:3	$CDCl_3$	21	138	**3.8c-o**	0[b]

[a] Expressed as the molar ratio of diene to dienophile. [b] Yields determined by ^{1}H NMR spectroscopy.

Dithienylfuran compounds **3.6a** and **3.6c** were screened for the ability to form DA adducts using a third dienophile, tetracyanoethylene (Table 3.3). Solu-

tions containing the diphenyl derivative **3.6a** again formed intensely coloured mixtures immediately upon treatment with the dienophile (Figure 3.2), and ^{1}H NMR and UV-vis absorbance spectra obtained from the mixtures again suggested that the colouration was likely due to formation of a charge transfer complex as opposed to the DA adduct **3.9a-o**. No reaction was observed between the diester compound **3.6c** and tetracyanoethylene despite attempts to vary the reaction temperatures and reagent stoichiometries.

Table 3.3 Screening of dithienylfuran compounds for DA adduct formation with tetracyanoethylene.

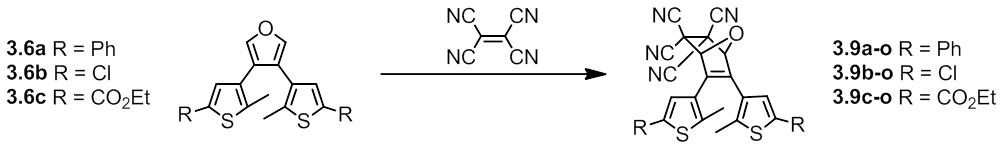

diene	*stoichiometry*[a]	*solvent*	*temperature* / °C	*time* / h	*product*	*yield* / %
3.6a	1:1	$CDCl_3$	21	24	**3.9a-o**	0[b]
3.6c	1:1	$CDCl_3$	70	24	**3.9c-o**	0[b]
3.6c	1:1	$CDCl_3$	40	24	**3.9c-o**	0[b]
3.6c	1:3	$CDCl_3$	21	94	**3.9c-o**	0[b]

[a] Expressed as the molar ratio of diene to dienophile. [b] Yields determined by ^{1}H NMR spectroscopy.

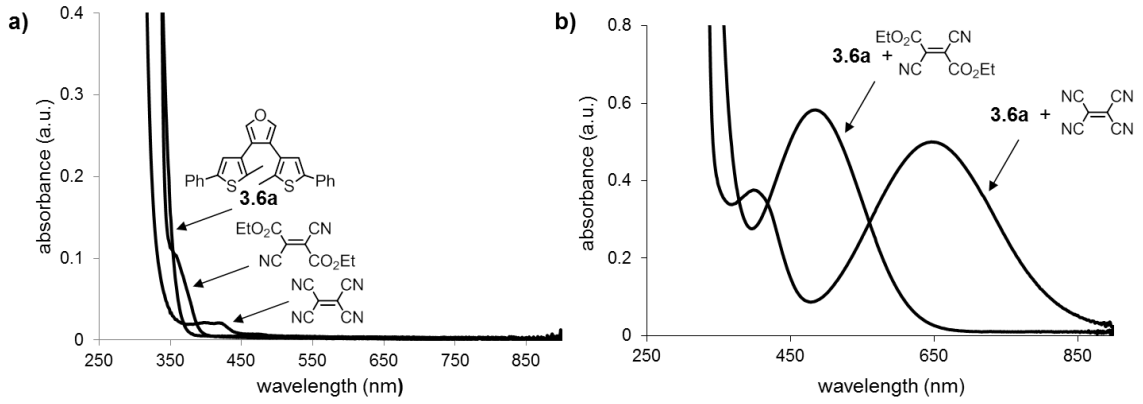

Figure 3.2 (a) UV-vis absorbance spectra acquired from compound **3.6a**, diethyldicyanofumarate, and tetracyanoethylene, and (b) spectra acquired from mixtures of **3.6a** with diethyldicyanofumarate and **3.6a** with tetracyanoethylene. All spectra were obtained from 30 mM $CHCl_3$ solutions at 20 °C.

3.3.3 Photochemical Screening

Each of the two DA adducts that had formed was further screened based on its ability to undergo photochemical ring-closing and ring-opening reactions upon exposure to UV and visible light, respectively. UV-vis absorbance spectra obtained from a solution of compound **3.7b-o** (Figure 3.3) indicate development of a visible absorbance band centred at 440 nm following irradiation with 313 nm light, which is consistent with photochemical ring-closure (see Section 1.2.1). However, the lack of an observable isosbestic point (*i.e.* a point where all of the spectra acquired over the course of the reaction intersect) suggests that irradiation leads to the formation of additional species (*i.e.* other compounds besides **3.7b-o** and **3.7b-c**) that contribute to the absorbance spectra. This was verified by monitoring the intensity of the absorbance band corresponding to the ring-closed isomer during repeated photochemical cycling between the ring-open and ring-closed isomers (Figure 3.2, inset), which was carried out by alternately irra-

diating a solution of compound **3.7b-o** with UV (*i.e.* 313 nm, 40 s) and visible light (*i.e.* >450 nm, 120 s). The results depict a decrease in the maximum absorbance and an increase in the minimum absorbance after just four cycles, which is consistent with degradation of **3.7b-c** and formation of one or more compounds that absorb more strongly than **3.7b-o** at 440 nm.

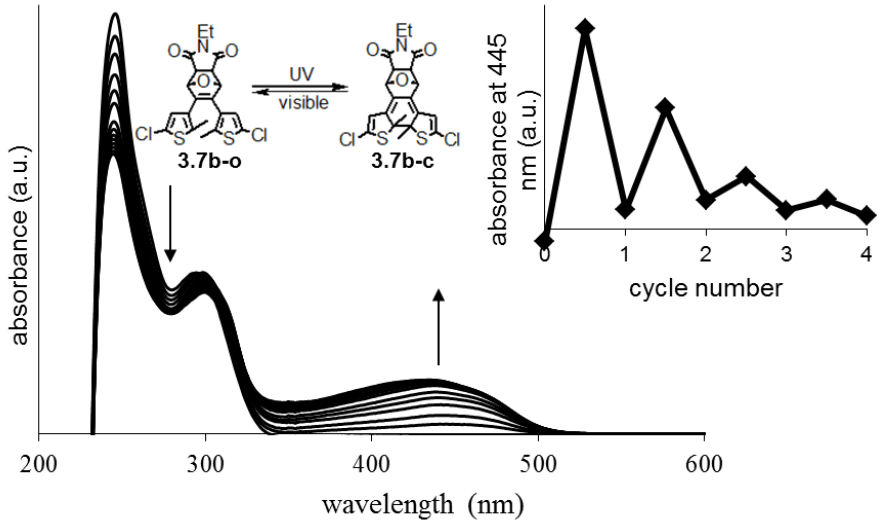

Figure 3.3 Photochemical conversion of compound **3.7b-o** to ring-closed isomer **3.7b-c** *via* irradiation with 313 nm light; monitored by UV-vis absorbance spectra acquired in CH_2Cl_2 (1.0×10^{-5} M, 20° C) over 5 s intervals. Arrows indicate the directions of spectral changes corresponding to increasing amounts of UV light exposure. The inset plot depicts changes in absorbance at the visible wavelength maximum accompanying alternating periods of exposure to UV (40 s) and visible light of wavelengths greater than 450 nm (120 s).

The attempted conversion of **3.7b-o** to its corresponding ring-closed isomer was also monitored by ^{1}H NMR spectroscopy in order to verify the structure of the photochemical reaction product and to estimate PSS_{313} (Figure 3.4). Irradiation with UV light led to a progressive decrease in intensities of the singlets attributable to thienyl protons H_a and succinimidyl protons H_d in the ring-open compound **3.7b-o**. This was accompanied by the appearance of two singlets cor-

responding to the diastereotopic thienyl protons, H_b and H_c, and two doublets attributable to the diastereotopic succinimidyl protons, H_e and H_f, in the ring-closed isomer **3.7b-c**. Both sets of signals appear at higher-field (*i.e.* lower ppm) in the case of the ring-closed compound due to the loss of thiophene aromaticity accompanying ring-closure.

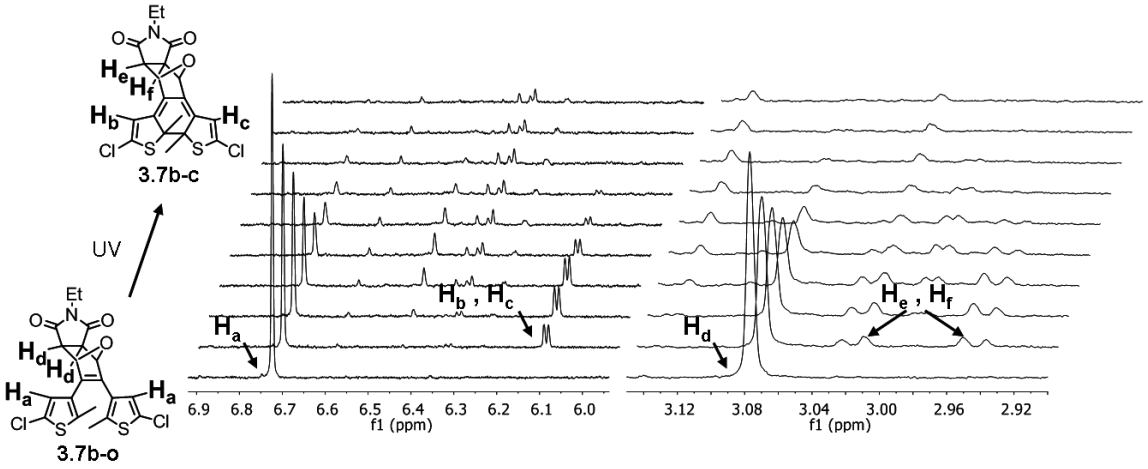

Figure 3.4 Partial ^{1}H NMR spectra acquired in two-minute intervals during irradiation of compound **3.7b-o** in CD_2Cl_2 with 313 nm light.

Increasing irradiation time also led to the appearance of many low-intensity peaks attributable to neither of the two compounds. This is consistent with the observation that the sum of the integrated signals corresponding to H_a, H_b and H_c (*i.e.* as well as the sum of the integrated signals arising from H_d, H_e and H_f) decreases with irradiation time (Figure 3.5), which indicates that the reversible photoisomerization is accompanied by one or more irreversible chemical reactions. However, the new signals were too numerous and weak to reliably identify any of the degradation products. The rate of degradation was nevertheless sufficient to prevent compounds **3.7b-o** and **3.7b-c** from reaching photo-

chemical equilibrium, making it impossible to determine PSS_{313} directly *via* NMR spectroscopy.

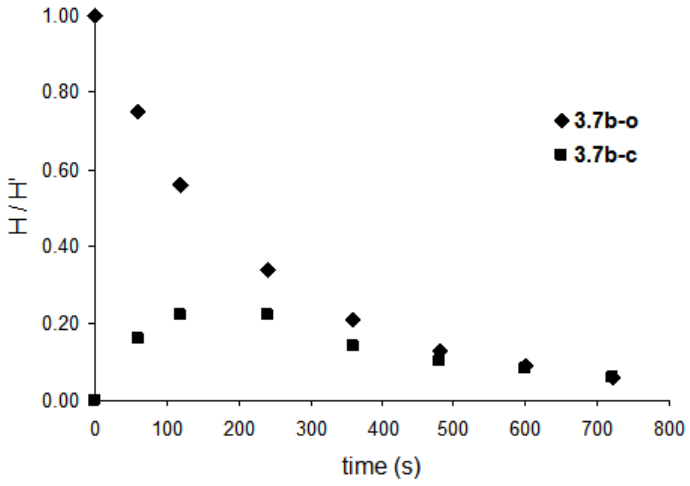

Figure 3.5 Concentrations of **3.7b-o** (diamonds) and **3.7b-c** (squares) expressed as functions of time, during which a mixture of the two compounds in CD_2Cl_2 was irradiated with 313 nm light. Concentrations are expressed as fractions of the amount of **3.7b-o** present before irradiation (*i.e.* at time t = 0 s), which were determined *via* integration of the ^{1}H NMR signals attributed to protons labeled H_d, H_e and H_f in Figure 3.3.

UV-vis absorbance spectra acquired during irradiation of diester adduct **3.7c-o** (10 μM in CH_3CN, 20° C) revealed the development of bands centred at 350 nm and 520 nm as the intensity of the band centred at 255 nm decreases (Figure 3.5). These phenomena are consistent with conversion of the ring-open isomer to compound **3.7c-c**. It is noteworthy that the superimposed spectra contain an isosbestic point at approximately 315 nm, which suggests that few side-products, if any, are generated during photoisomerization. This is supported by UV-vis absorbance data obtained during repeated photochemical cycling of the compound between its ring-open and ring-closed isomers, which indicate little change in the minimum and maximum absorbance values measured at 520 nm

(*i.e.* the amounts of ring-open and ring-closed compound remain nearly constant throughout the photochemical cycling studies).

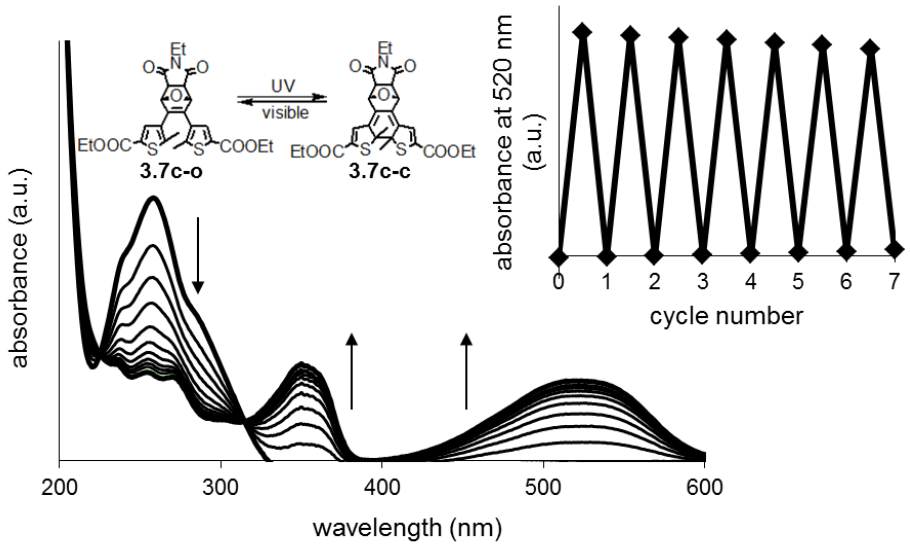

Figure 3.6 Photochemical conversion of compound **3.7c-o** to ring-closed isomer **3.7c-c** *via* irradiation with 313 nm light, monitored by UV-vis absorbance spectra acquired in CH_3CN over 5 s intervals (1.0×10^{-5} M, 20° C). Arrows indicate the directions of spectral changes corresponding to increasing amounts of UV light exposure. The inset plot depicts changes in absorbance at the visible wavelength maximum accompanying alternating periods of exposure to 313 nm light (40 s) and visible light of wavelengths greater than 450 nm (120 s).

Photochemical conversion of compound **3.7c-o** to its ring-closed isomer was also monitored by ^{1}H NMR spectroscopy (Figure 3.7). Irradiation with 313 nm light led to decreasing intensities of the singlets attributable to thienyl protons H_a and succinimidyl protons H_d in the ring open isomer. These changes were accompanied by the appearance of two singlets corresponding to diastereotopic thienyl protons H_b and H_c and two doublets arising from diastereotopic succinimidyl protons H_e and H_f in the ring-closed isomer. As with the dichloro adduct, signals arising from the ring-closed compound appeared at higher field than their ring-open counterparts.

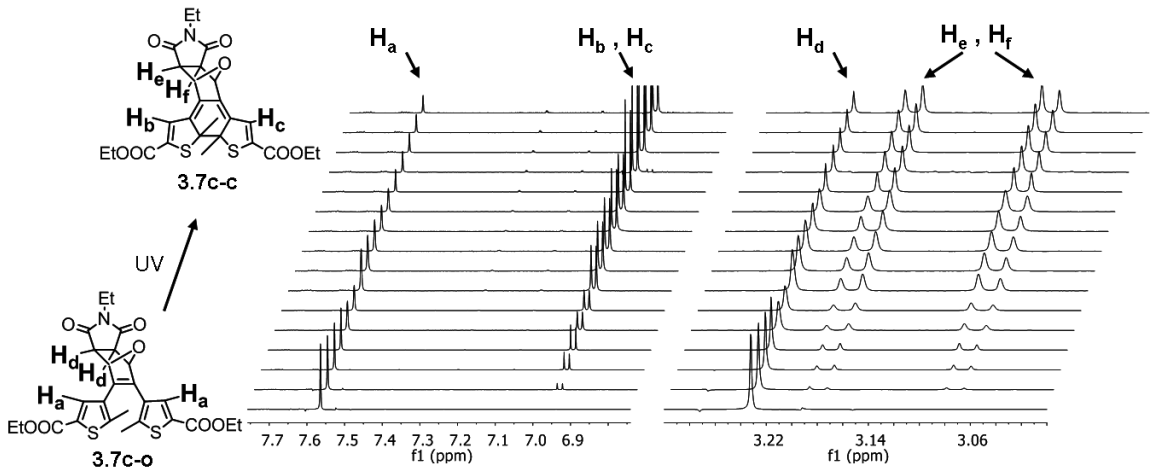

Figure 3.7 Partial ^{1}H NMR spectra acquired in two-minute intervals during irradiation of compound **3.7c-o** in CD_3CN with 313 nm light.

Unlike the dichlorinated compound **3.7b-o**, increased exposure of diester adduct **3.7c-o** to UV light led only to the appearance of signals corresponding to the ring-closed structure. Integration of the signals attributable to H_d, H_e and H_f revealed that the sum of the concentrations of **3.7c-o** and **3.7c-c** remained roughly the same throughout the experiment (Figure 3.8). These data are typical for a reversible, first-order reaction[70] and are consistent with the UV-vis absorbance spectra shown in Figure 3.6, which suggest little, if any, photodegradation during ring-closure or repeated cycling between the two isomers. PSS_{313} was reached after irradiation of the mixture for 30 minutes and found to consist of approximately 88% **3.7c-c** and 16% **3.7c-o**.

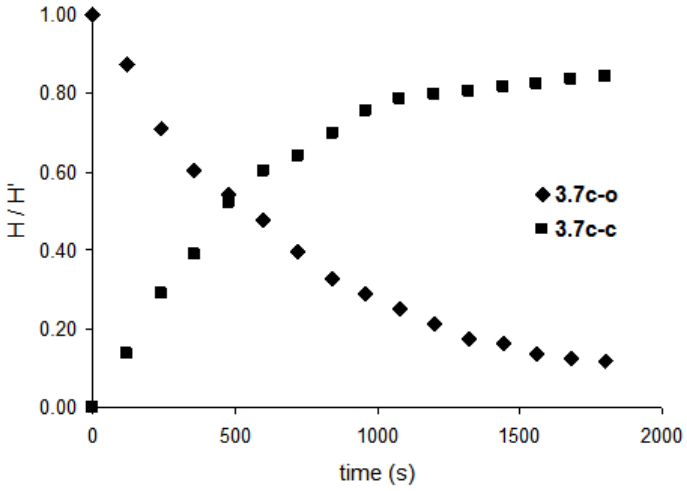

Figure 3.8 Concentrations of **3.7c-o** (diamonds) and **3.7c-c** (squares) expressed as functions of time, during which a mixture of the two compounds in CD_3CN was irradiated with 313 nm light. Concentrations are expressed as fractions of the amount of **3.7c-o** present before irradiation (*i.e.* at time t = 0 s), which were determined *via* integration of the ^{1}H NMR signals attributed to protons labeled H_d, H_e and H_f in Figure 3.6.

3.3.4 Retro-DA Reaction

The ability of **3.7c-o** to selectively undergo the retro-DA reaction in the presence of **3.7c-c** was investigated by comparing ^{1}H NMR spectra acquired from a 1:1 mixture of the two isomers in DMSO-d_6 before (Figure 3.8a) and after (Figure 3.8b) heating at 100° C for 24 h. In addition to signals present in the parent mixture, the spectrum obtained after heating was found to contain new signals attributable to dithienylfuran **3.6c** (Figure 3.8c) and *N*-ethylmaleimide (Figure 3.8d), indicating that the retro-DA reaction had taken place. However, the intensities of the signals arising from the ring-open photoisomer were the only ones seen to decrease, suggesting that the retro-DA reaction occurred solely from compound **3.7c-o**. Analysis of the signal integrals corresponding to each compound confirmed that the amount of **3.7c-o** consumed (*i.e.* in moles) was shown

to equal the amounts of **3.6c** and N-ethylmaleimide that had formed, further supporting the conclusion that the ring-open adduct was converted to its parent diene and dienophile while the ring-closed compound remained intact.

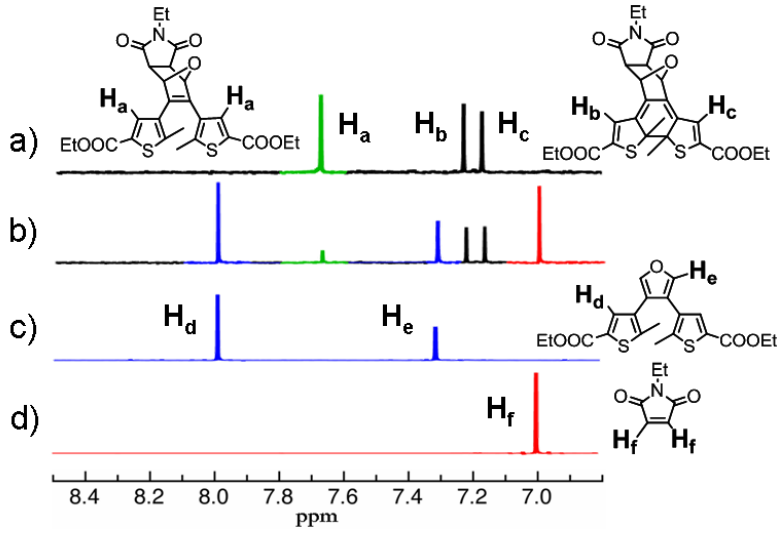

Figure 3.9 Partial ^{1}H NMR spectra acquired from a 1:1 mixture of **3.7c-o** and **3.7c-c** in DMSO-d_6 (a) before and (b) after heating at 100° C for 24 h, as well as partial ^{1}H NMR spectra of (c) compound **3.6c** and (d) N-ethylmaleimide acquired in the same solvent.

3.4 **Conclusion**

3.4.1 Summary

A series of 3,4-dithienylfuran compounds was synthesized and screened for the ability to undergo the DA reaction with various dienophiles. The two DA adducts that formed were then isolated and further screened for efficient, reversible photoisomerization, a criterion satisfied only by diester adduct **3.7c-o**. The diester adduct was shown to exhibit a difference in its ability to undergo the retro-DA reaction depending on whether it was present as the ring-open or ring-closed photoisomer. Exposing a mixture of the two photoisomers to elevated

temperatures (*i.e.* 100° C) led to the thermolysis of the ring-open compound and regeneration of its parent diene and dienophile, during which the ring-closed isomer remained intact. These results highlight the reversible conversion of adduct **3.7c-o** to its corresponding ring-closed photoisomer as a potentially valuable motif for expanding the range of working environments available to thermoresponsive systems based on the DA reaction.

3.4.2 Prospective and Ongoing Research

Ongoing research is primarily focused on evaluating the photo-gated DA reaction between dithienylfuran **3.6c** and *N*-alkylmaleimides as a means to mitigate the loss of mechanical strength in self-healing polymers at elevated temperatures. Reports of ring-opening metathesis polymerization (ROMP) performed on dithienylethenes[71,72] suggest that an analogous approach could be used to generate polymer **3.15** from dithienylfuran monomer **3.14** (Scheme 3.11). Solutions of **3.15** treated with varying amounts of a bifunctional or trifunctional maleimide cross-linker could then be spin-coated onto quartz slides, yielding thin-films suitable for characterization of the subsequent cross-linking and photoisomerization reactions *via* UV-vis absorbance spectroscopy. Differential scanning calorimetry (DSC) could then be used to monitor the occurrence of the retro-DA reaction in films prepared from **3.16-o** and **3.16-c** based on whether endothermic peaks are observed while heating. The ability of each polymer film to undergo spontaneous self-healing can be investigated by examining the surface of the material *via* scanning electron microscopy (SEM) at varying intervals after scratching or scraping the polymer film. Finally, the mechanical strength of each polymer film

at elevated temperatures can then assessed in terms of its elastic modulus, which can be measured using the micro-cantilever method described by McShane *et. al.*[73]

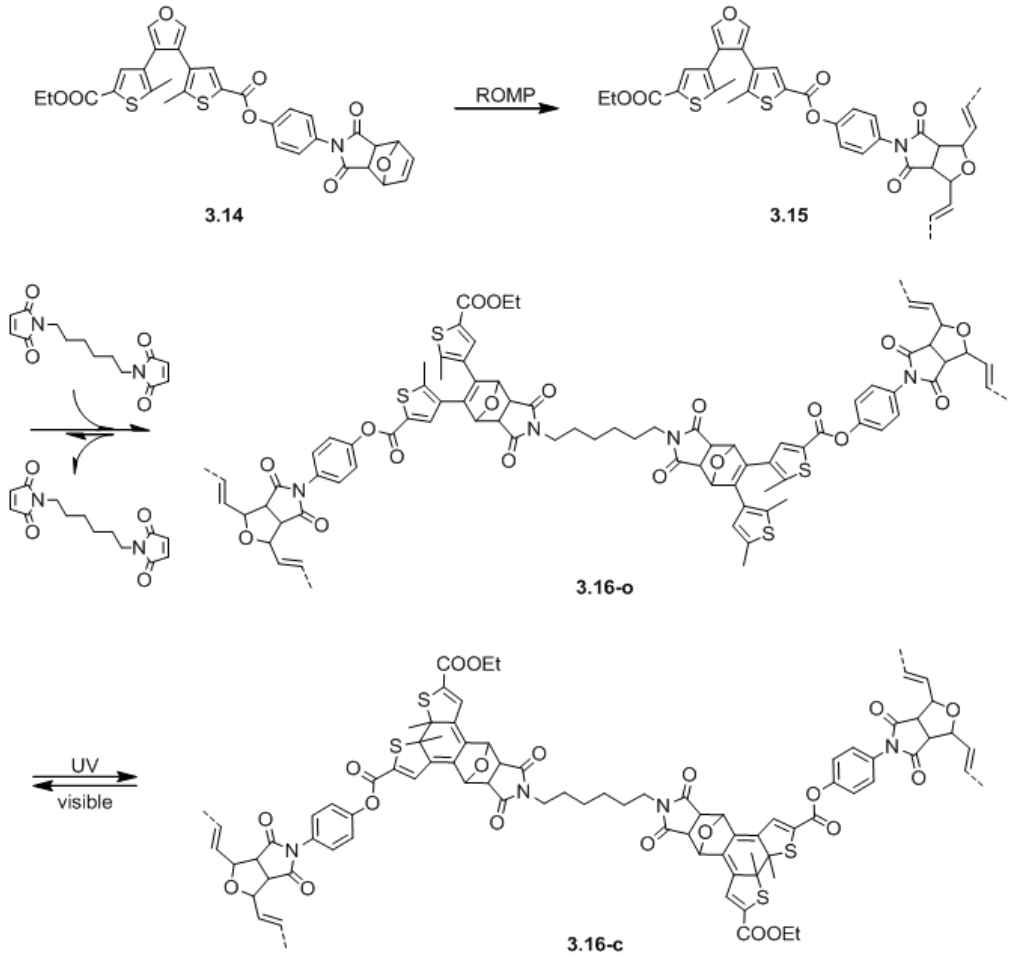

Scheme 3.11 Preparation of a photoresponsive, self-healing polymer *via* ROMP, DA reaction with a bifunctional maleimide cross-linker, and UV photoisomerization.

3.5 **Experimental**

3.5.1 Materials

Unless otherwise noted, all solvents used for synthesis and UV-vis spectroscopy were purchased from Fisher or Aldrich and, except for tetrahydrofuran and diethyl ether, used without further purification. THF and Et_2O were dried over sodium metal and distilled under N_2. Solvents for NMR spectroscopy were purchased from Cambridge Isotope Laboratories and used as received. Reagents and synthetic starting materials were purchased from Aldrich and used without further purification. 3,4-Dibromofuran (**3.10**) was synthesized following a procedure reported in Reference 57. Bromothiophenes **3.12a** and **3.12b** were synthesized according to literature procedures,[36,59] as were thiopheneboronic acids **3.13a** and **3.13b**.[60]

3.5.2 Instrumentation

All synthetic precursors to compounds **3.7b-o** and **3.7c-o** were characterized by ^{1}H NMR and ^{13}C NMR spectroscopy performed using a Bruker AVANCE 400 BBOF direct probe working at 400.13 MHz and 100.62 MHz for ^{1}H and ^{13}C NMR spectra, respectively. Characterization of compounds **3.6a**, **3.7b-o** and **3.7c-o**, as well as the photoisomerization and retro-DA reaction studies were carried out using a Bruker AVANCE 500 TXI inverse $^{1}H/^{13}C/^{19}F$ probe working at 500.19 MHz and 125.78 MHz for ^{1}H and ^{13}C NMR spectra, respectively. Chemical shifts are reported in parts per million relative to TMS using the residual solvent peak as a reference standard. Coupling constants are reported in hertz. UV-vis absorbance measurements were performed using a Varian Cary 300 Bio

Spectrometer, and mass spectrometry measurements were performed using an Agilent 6210 TOF LC/MS.

3.5.3 Photochemistry

Ring-closing reactions were carried out with 313 nm light from a handheld UV lamp (Spectroline E-Series, 3.5 mW cm^{-2}). Ring-opening reactions were performed using light from a 300 W tungsten source passed through a 450 nm cutoff filter. Photoreactions monitored by UV-vis spectroscopy were performed on 10 μM solutions in 1 cm quartz cuvettes (*e.g.* CH_2Cl_2 was used in the case of **3.7b-o**, and CH_3CN was used in the case of **3.7c-o**). Ring-closing reactions were typically carried out for 40 s and ring-opening reactions were carried out for 120 s.

3.5.4 Synthesis

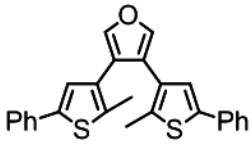

3.6a

Synthesis of compound (3.6a)

A solution of (2-methyl-5-phenylthiophen-3-yl)boronic acid (**3.13a**) (0.70 g, 3.1 mmol) in THF (25 mL) was treated with 3,4-dibromofuran (**3.10**) (0.34 g, 1.6 mmol) and saturated, aqueous $Na_2CO_3 \bullet H_2O$ (20 mL). The resulting suspension was deoxygenated with a stream of N_2 and treated with $Pd(PPh_3)_4$ (110 mg, 0.093 mmol). The mixture was heated at reflux while stirring magnetically for 66 hours, after which the heating source was removed and the reaction mixture allowed to cool to room temperature. Et_2O (50 mL) was added to the mixture, and

the layers were separated. The aqueous layer was extracted with Et_2O (3 x 20 mL), and the combined organic layers dried over $MgSO_4$ and filtered. The filtrate was adsorbed onto silica gel and concentrated to dryness *in vacuo*. The adsorbed mixture was purified by flash column chromatography on silica (neat hexane), affording 200 mg (31%) of compound **3.6a** as a white solid.

M.p. = 43-45° C. ^{1}H NMR (500 MHz, $CDCl_3$, *δ*): 7.56 (dd, *J* = 8.4, 1.3 Hz, 4H), 7.36 (tt, *J* = 7.4, 1.5 Hz, 4H), 7.25 (tt, *J* = 7.4, 1.2 Hz, 2H), 7.12 (s, 1H), 7.11 (s, 1H), 6.74 (dd, *J* = 2.3, 1.2 Hz, 1H), 6.73 (dd, *J* = 2.3, 1.2 Hz, 1H), 2.53 (s, 3H), 2.52 (s, 3H). ^{13}C NMR (125 MHz, $CDCl_3$, δ): 142.1, 139.6, 134.8, 128.9, 127.1, 126.3, 125.6, 123.0, 15.5.

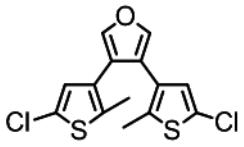

3.6b

Synthesis of compound (3.6b)

A solution of (5-chloro-2-methylthiophen-3-yl)boronic acid (**3.13b**) (1.18 g, 6.70 mmol) in DMF (25 mL) was treated with 3,4-dibromofuran (**3.10**) (608 mg, 3.00 mmol) and Na_2CO_3•H_2O (2.0 g, 16.0 mmol). The resulting suspension was purged for 1.5 h with a stream of N_2 and treated with $Pd(PPh_3)_4$ (93 mg, 0.080 mmol). The mixture was heated at 110° C and stirred magnetically for 52 h, after which the heating source was removed and the reaction allowed to cool to room temperature. Water (100 mL) was added and the suspension extracted with Et_2O (3 x 50 mL). The combined organic layers were dried over $MgSO_4$ and filtered.

The filtrate was adsorbed onto silica gel and concentrated to dryness *in vacuo*. The adsorbed mixture was purified by flash column chromatography on silica (neat hexanes), affording colourless crystals that rapidly developed a yellow/brown hue upon exposure to light and oxygen at ambient temperatures. Recrystallization from CH_2Cl_2 and hexane under reduced pressure yielded colourless crystals of compound **3.6b** once more (451 mg, 46%), which were stored at -20° C in the dark.

M.p. = 81-83° C. ^{1}H NMR (500 MHz, $CDCl_3$, δ): 7.43 (s, 2H), 6.49 (s, 2H), 2.14 (s, 6H). ^{13}C NMR (125 MHz, CDCl3, δ): 147.9, 140.9, 134.4, 127.7, 125.7, 120.2, 13.8. HRMS (CI) *m/z* calculated for $C_{14}H_{11}Cl_2OS_2$ ($M+H^+$) 328.9, found 329.2.

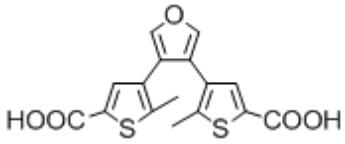

Synthesis of 4,4′-(furan-3,4-diyl)*bis*(5-methylthiophene-2-carboxylic acid)

A stirred solution of 3,4-*bis*(5-chloro-2-methylthiophen-3-yl)furan (**3.6b**) (135 mg, 0.410 mmol) in anhydrous Et_2O (10 mL) was cooled to -78° C under N_2 and was treated with *t*-BuLi in pentane (1.5 M, 1.0 mL, 1.5 mmol), added dropwise over 5 min. The reaction was stirred under N_2 for 1.5 h at -78° C, after which gaseous CO_2 (sublimed from solid CO_2 and passed through a drying tube filled with Drierite) was bubbled under the surface of the stirring reaction mixture, forming a white precipitate, and the temperature maintained for 3 h. The cooling bath was then removed and the reaction mixture allowed to warm to room

temperature. After 1 h, the mixture was treated with aqueous HCl (10%, 10 mL), which caused the precipitate to dissolve. The mixture was washed with water (25 mL) and the layers separated. The aqueous layer was extracted with Et_2O (2 x 20 mL) and the combined organic layers extracted with aqueous NaOH (2.5 M, 2 x 100 mL). The combined aqueous layers were stirred magnetically and treated dropwise with concentrated HCl until the pH of the mixture was below 1. The white precipitate that formed was then isolated by suction filtration and washed with water. The crude solid was purified by flash column chromatography on silica (9:1:0.01 CH_2Cl_2:MeOH:AcOH) affording the dicarboxylic acid as a white solid (88 mg, 62%).

M.p. = 250° C (decomposed). ^{1}H NMR (500 MHz, CD_3OD, *δ*): 7.63 (s, 2H), 7.25 (s, 2H), 2.18 (s, 6H). ^{13}C NMR (125 MHz, CD_3OD, δ): 225.6, 182.1, 163.8, 161.8, 155.2, 150.0, 140.1, 33.7. HRMS (ESI+) *m/z* calculated for $C_{16}H_{13}O_5S_2$ ($M+H^+$) 349.0199, found 349.0199.

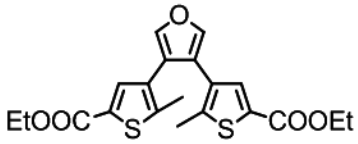

3.6c

Synthesis of compound (3.6c)

A solution of 4,4′-(furan-3,4-diyl)*bis*(5-methylthiophene-2-carboxylic acid) (57 mg, 0.16 mmol) in anhydrous EtOH (25 mL) was treated with 5 drops of concentrated H_2SO_4. The reaction mixture was heated to reflux and stirred magnetically under N_2 for 17 h, after which the heat source was removed and the reaction mixture allowed to cool to room temperature. Water (50 mL) was added

and the resulting mixture extracted with CH_2Cl_2 (3 x 50 mL). The combined organic layers were dried over $MgSO_4$, filtered and concentrated to dryness *in vacuo*. The residue was purified by flash column chromatography on silica (neat CH_2Cl_2), affording compound **3.6c** as a colourless, crystalline solid (46 mg, 70%).

^{1}H NMR (500 MHz, $CDCl_3$, *δ*): 7.50 (s, 2H), 7.38 (s, 2H), 4.28 (q, *J* = 7.1 Hz, 4H), 2.19 (s, 6H), 1.33 (t, *J* = 7.0 Hz, 6H). ^{13}C NMR (125 MHz, $CDCl_3$, *δ*): 161.1, 143.6, 140.9, 135.0, 129.8, 129.5, 120.2, 60.9, 29.6, 14.4, 14.2. HRMS (CI) *m/z* calculated for $C_{20}H_{24}NO_5S_2$ ($M+NH_4^+$) 422.1090, found 422.1107.

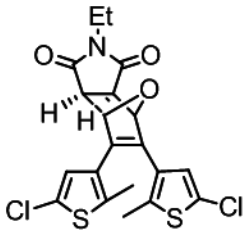

3.7b-o

Synthesis of compound (3.7b-o)

A solution of 3,4-*bis*(5-chloro-2-methylthiophen-3-yl)furan (**3.6b**) (18 mg, 0.055 mmol) in $CDCl_3$ (0.60 mL) was treated with *N*-ethylmaleimide (7.0 mg, 0.055 mmol) and the mixture transferred to an NMR tube. The NMR tube was heated at 70° C for 73 h, after which the reaction mixture was concentrated to dryness *in vacuo* and the residue purified by flash column chromatography on silica (CH_2Cl_2), affording compound **3.7b-o** as a colourless, crystalline solid (20 mg, 79%).

M.p. = 166-167° C. ^{1}H NMR (500 MHz, $CDCl_3$, *δ*): 6.67 (s, 2H), 5.35 (s, 2H), 3.55 (q, *J* = 7.2 Hz, 2H), 3.06 (s, 2H), 1.95 (s, 6H), 1.17 (t, *J* = 7.2 Hz, 3H).

^{13}C NMR (125 MHz, $CDCl_3$, *δ*): 176.0, 138.9, 136.9, 129.4, 127.4, 126.2, 85.6, 48.9, 34.4, 30.2, 14.8, 13.2. HRMS (CI) *m/z* calculated for $C_{20}H_{18}Cl_2NO_3S_2$ ($M+H^+$) 454.0100, found 454.0110.

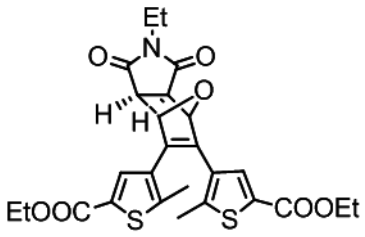

3.7c-o

Synthesis of compound (3.7c-o)

To a solution of diethyl 4,4′-(furan-3,4-diyl)*bis*(5-methylthiophene-2-carboxylate) (**3.6c**) (20 mg, 0.049 mmol) in $CDCl_3$ (0.60 mL) was added *N*-ethylmaleimide (6.2 mg, 0.049 mmol), and the mixture was transferred to an NMR tube. The reaction mixture was heated to 70° C for 38 h, after which the heat source was removed and the reaction allowed to cool to room temperature. The crude mixture was concentrated to dryness *in vacuo* and the residue purified by flash column chromatography on silica (5% EtOAc in CH_2Cl_2) affording compound **3.7c-o** as a colourless, crystalline solid (17 mg, 65%).

M.p. = 78-81° C. ^{1}H NMR (500 MHz, CD_3CN, *δ*): 7.56 (s, 2H), 6.38 (s, 2H), 4.28 (q, *J* = 7.1 Hz, 4H), 3.47 (q, *J* = 7.2 Hz, 2H), 3.23 (s, 2H), 2.01 (s, 6H), 1.31 (t, *J* = 7.1 Hz, 3H). ^{13}C NMR (125 MHz, CD_3CN, *δ*): 177.2, 162.8, 146.4, 140.3, 134.3, 132.3, 132.1, 86.3, 62.5, 49.5, 34.8, 15.6, 14.9, 13.6. HRMS (ESI+) *m/z* calculated for $C_{26}H_{28}NO_7S_2$ ($M+H^+$) 530.1302, found 530.1338.

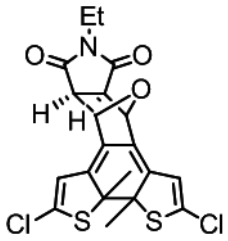

3.7b-c

Synthesis of compound (3.7b-c)

A solution of compound **3.7b-o** in CD_2Cl_2 (0.60 mL, 1.5 mM) was transferred to an NMR tube and irradiated with 313 nm light for 1 min, after which its ^{1}H NMR spectrum was recorded. Irradiation was continued and new ^{1}H NMR spectra were recorded in 2 min intervals until the reaction mixture, which had gone from colourless to pale yellow, had been irradiated for a total of 16 min. Further irradiation led to formation of increasing amounts of uncharacterized side products. The ring-closed compound was not isolated.

^{1}H NMR (500 MHz, CD_2Cl_2, δ): 6.11 (s, 1H), 6.10 (s, 1H), 5.23 (s, 1H), 5.19 (s, 1H), 3.49-3.54 (m, 2H), 3.01 (d, J = 6.6 Hz, 1H), 2.94 (d, J = 6.8 Hz, 1H), 1.98 (s, 3H), 1.93 (s, 3H), 1.14 (m, 3H).

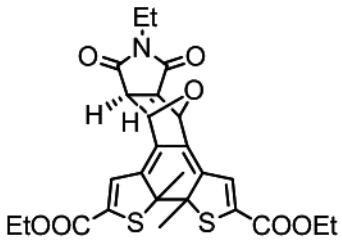

3.7c-c

Synthesis of compound 3.7c-c

A solution of compound **3.7c-o** in CD_3CN (0.60 mL, 19 mM) was transferred to an NMR tube and irradiated with 313 nm light for 2 minutes, after

which its ^{1}H NMR spectrum was recorded. Irradiation was continued and new ^{1}H NMR spectra were recorded in 2 min intervals until the reaction mixture, which had gone from colourless to red, had been exposed to 313 nm light for a total of 30 min. PSS_{313} was found to consist of 88% **3.7c-c** and 12% **3.7c-o**.

^{1}H NMR (500 MHz, CD_3CN, δ): 6.95 (s, 1H), 6.93 (s, 1H), 5.35 (s, 1H), 4.22-4.25 (m, 4H), 3.43-3.47 (m, 2H), 3.18 (d, J = 6.8 Hz, 1H), 3.07 (d, J = 6.8 Hz, 1H), 1.96 (s, 3H), 1.95 (s, 3H), 1.27-1.30 (m, 6H), 1.06-1.09 (m, 3H).

3.5.5 Retro-DA Reaction

Thermolysis of isomers 3.7c-o and 3.7c-c

A solution of compound **3.7c-o** in DMSO-d_6 (0.60 mL, 0.10 mM) was irradiated with 313 nm light for 50 s and its ^{1}H NMR spectrum recorded, confirming the presence of equal amounts of **3.7c-o** and **3.7c-c**. The NMR tube was protected from light and heated to 100° C, and the composition of the reaction mixture was analyzed by ^{1}H NMR spectroscopy in 24 h intervals. After 72 h, no further changes to the spectra were observed. The concentrations of **3.7c-o**, *N*-ethylmaleimide and **3.6c** present were found to be 3%, 97% and 97% of the concentration of **3.7c-o** measured prior to heating. In contrast, the concentration of compound **3.7c-c** remained constant throughout the experiment. These percentages were calculated based on the assumption that **3.7c-o**, **3.7c-c**, **3.6c**, and *N*-ethylmaleimide were the only reactive components in the mixture. A separate experiment, performed using 1,4-dibromobenzene as an inert, internal integration standard, confirmed the validity of this assumption (*i.e.* the

concentration of **3.7c-c** remained constant relative to the concentration of 1,4-dibromobenzene).

CHAPTER 4: CONCLUSION

4.1 Objectives

Using light to control materials offers degrees of spatial, temporal, and chemical selectivity superior to those resulting from electrical stimuli or changes in temperature. However, designing materials that respond to optical stimuli in a desired fashion can be challenging, given the need for such materials to efficiently absorb particular wavelengths of light and undergo excited state deactivation predominantly *via* a preferred pathway. These challenges can be mitigated by design strategies that integrate molecular photoswitching motifs based on dithienylethenes, which undergo a bidirectional transformation when exposed to light of different wavelengths (*i.e.* UV light elicits ring-closure, visible light elicits ring-opening). By coupling the structural and electronic features distinct to either form with secondary physical or chemical events, it is possible to control those events by interconversion of the two dithienylethene isomers using complementary optical stimuli (*e.g.* UV and visible light). The studies described in Chapters 2 and 3 apply these principles, introduced in Chapter 1, to the control of luminescent and thermoresponsive materials.

4.2 Controlling Luminescent Materials

The ability to control light-emitting materials using a second stimulus (*i.e.* the first stimulus is used to electronically excite the lumophore) is beneficial to chemo- and biosensor design, as well as imaging and prospective data storage

technologies. Control *via* a second stimulus is typically achieved by manipulating the viability of energy transfer or electron transfer interactions between the lumophore and an associated quenching moiety, a paradigm that readily lends itself to molecular photoswitching motifs.

Several examples have been developed in which switch molecules held in close proximity to light-emitting components provide different quenching efficiencies depending on whether the switch is present in its corresponding ring-open or ring-closed form. However, these examples are fraught with a variety of limitations related to the choice of lumophore and quencher design. Chapter 2 describes a modified design intended to address these limitations, a design that consists of a cationic dithienylethene quencher coordinated to the surface of a CdSe-ZnS quantum dot. The synthesis of the dithienylethene and its subsequent coordination to the QD surface *via* ligand exchange are reported, as well as confirmation of photochemically gated luminescence quenching and efforts to elucidate the underlying mechanisms.

Preparation of the functionalized QDs, though successful, was problematic due to a noteworthy decrease in QD stability during the ligand exchange reaction, which led to extensive aggregate formation and material losses. This may have been due to disproportionate loss of stabilizing TOPO ligands during removal of excess, unbound dithienylethene molecules and might have been remedied by including additional TOPO during successive purification steps (*i.e.* excess TOPO would likely have done little to interfere with subsequent UV-vis absorbance or luminescence measurements).

Spectroscopic measurements performed on the functionalized QDs succeeded in confirming the ability to toggle QD luminescence between high-intensity and low-intensity states by interconversion of the coordinated dithienylethene between its corresponding ring-open and ring-closed photoisomers. Both states exhibit significant quenching, however, with 88% of the QD emission quenched by the ring-open isomer and 96% quenched by the ring-closed. Spectral overlap between the UV-vis absorbance bands of the ring-open and ring-closed dithienylethenes with the QD emission band lead to projected FRET efficiencies of 1.3% and 33%, respectively, which suggest additional luminescence quenching *via* a second mechanism. The reduction potentials of the two unbound dithienylethene photoisomers were determined by cyclic voltammetry and used to calculate ΔG° values corresponding to the possibility of luminescence quenching due to photoinduced electron transfer. The values obtained are consistent with the observed luminescence data, suggesting that electron transfer to the ring-open isomer is slightly endergonic (+0.57 meV), whereas electron transfer to the ring-closed isomer is noticeably more exergonic (-320 meV).

Repeated toggling between the high-intensity and low-intensity states revealed a gradual decrease in the maximum QD emission and an increase in the minimum, which suggest progressive decomposition of the dithienylethene quencher. Given that the dithienylethene quencher had been tailored to function as an electron transfer acceptor, it is plausible that the resulting, neutral dithienylethene radical is gradually consumed *via* subsequent, irreversible chemical reactions. This is consistent with spectroscopic data acquired from the unbound

dithienylethene, which indicates greatly improved stability in the absence of an electron donor. It is also consistent with cyclic voltammetry data acquired from the unbound dithienylethene, which indicate that reduction is followed by an irreversible chemical reaction.

These observations constitute a significant shortcoming in the proposed system, severely limiting its potential utility in imaging and data storage applications. Addressing this flaw requires a better understanding of the underlying chemistry responsible for consumption of the neutral dithienylethene radical. Numerous reports regarding the stability of the analogous methyl viologen radical under comparable conditions suggest that consumption of the dithienylethene radical occurs *via* a different route. Identification of the major products resulting from this reaction, presumably simulated by large-scale electrolysis of the unbound dithienylethene, would constitute a necessary first step towards redesigning the quencher to improve its lifetime.

4.3 **Controlling Thermoresponsive Materials**

Emerging technologies based on thermoresponsive materials (*e.g.* self-healing polymers, cleavable surfactants, and dynamic combinatorial systems) offer a variety of attractive features. However, their usefulness is limited by the possibility of undesirable effects arising from accidental or unavoidable exposure to temperatures outside an intended regime. This shortcoming can be remedied by the use of optical stimuli as a means to toggle “off” and “on” the sensitivity of a thermoresponsive material to temperature.

Design motifs based on the Diels-Alder reaction are abundant among thermoresponsive systems due to its reversibility and sensitivity to temperature. Consequently, the studies described in Chapter 3 investigate the DA reaction between substituted dithienylfurans and various dienophiles as a means of constructing molecular switches capable of photochemically regulating the reversibility of the DA reaction over a range of temperatures.

Three dithienylfuran compounds were synthesized, bearing chloride, phenyl, and ester functional groups. The particular substituents were selected due to their synthetic accessibility and ability to provide a range of reactivities based on differences in electron-withdrawing and electron donating character. The dithienylfuran compounds were then screened for the ability to undergo the DA reaction with three dienophiles (*i.e. N*-ethylmaleimide, diethyldicyanofumarate, and tetracyanoethylene), which were selected on similar grounds.

Of the nine possible pairings only two led to the formation of DA adducts (*i.e.* the reactions of *N*-ethylmaleimide with the dithienylfuran compounds bearing chloride and ester substituents). Both compounds were formed exclusively as their corresponding *exo* isomeric forms, possibly due to steric interference of the thiophene rings with maleimide in the transition state geometry leading to the *endo* product. Two of the remaining seven pairings (*i.e.* the attempted reactions of diethyldicyanofumarate and tetracyanoethylene with the dithienylfuran compound bearing phenyl substituents) led to the rapid formation of highly coloured charge transfer complexes. Also, no attempt was made to react the chloro-substituted

dithienylfuran with either cyanoolefin based on the performance of the chloro-substituted adduct during photochemical screening (see below).

The two DA adducts were then screened for the ability to undergo bidirectional photoisomerization when exposed to UV and visible light. Both compounds formed their corresponding ring-closed isomers, however, isomerization of the chlorinated adduct was accompanied by rapid, irreversible decomposition (*i.e.* nearly all of the ring-open isomer had been consumed in just four cycles of ring-closure followed by ring-opening). In contrast, photoisomerization of the ester-substituted adduct proceeded cleanly, with few, if any, side products formed during either the forward or reverse reaction.

The ester-substituted DA adduct was then screened for the ability to selectively gate the reversibility of the DA reaction depending on whether the adduct was present in its ring-open or ring-closed form. A 1:1 mixture of the two isomers was examined by ^{1}H NMR spectroscopy after being heated at 100° C for 24 h, revealing formation of the corresponding diene and dienophiles in amounts proportional to the quantity of ring-open compound consumed. In comparison, the relative amount of ring-closed compound remained constant, confirming that ring-closure was effective in selectively preventing the occurrence of the retro-DA reaction.

These results encourage further investigation of thermoresponsive materials based on the DA reaction that incorporate carbonyldithienylfurans. In particular, the construction of self-healing polymers based on adducts of carbonyldithienylfuran with bifunctional maleimide cross-linkers are currently underway.

BIBLIOGRAPHY

[1] (a) Gregson, C. K. A. *et. al. J. Am. Chem. Soc.* **2006**, *128*, 7410. (b) Magenau, A. J. D.; Strandwitz, N. C.; Gennaro, A.; Matyjaszewski, K. *Science* **2011**, *332*, 81.

[2] Ho, R. J. Y.; Chien, J. Y. J. Pharm. Sci. 2009, 98, 1928.

[3] Huang, Z. Technol. Cancer Res. Treat. **2005**, 4, 283.

[4] Molecular Switches; Feringa, B. L., Ed.; Wiley-VCH: Weinheim, 2001.

[5] Irie, M. in *Organic Photochromic and Thermochromic Compounds*; Crano, J. C.;Gugliemetti, R. J., Eds.; Plenum: New York 1999; Vol. 1, pp 207.

[6] Bouas-Laurent, H.; Dürr, H. *Pure Appl. Chem.* **2001**, *73*, 639.

[7] Irie, M.; Lifka, T.; Uchida, K.; Seiya, K.; Shindo, Y. *Chem. Commun.* **1999**, 747.

[8] Higashiguchi, K. *et. al. Bull. Chem. Soc. Jpn.* **2000**, *73*, 2389.

[9] Hanazawa, M.; Sumiya, R.; Horikawa, Y.; Irie, M. *Chem. Commun.* **1992**, 206.

[10] Kellogg, R. M.; Groen, M. B.; Wynberg, H. *J. Org. Chem.* **1967**, *32*, 3093.

[11] Kitagawa, D.; Kobatake, S. *Chem. Lett.* **2011**, *40*, 93.

[12] Nakamura, S.; Irie, M. *J. Org. Chem.* **1988**, *53*, 6136.

[13] Irie, M.; Mohri, M. *J. Org. Chem.* **1988**, *53*, 803.

[14] Kobatake, S.; Uchida, K.; Tsuchida, E.; Irie, M. *Chem. Lett.* **2000**, 1340.

[15] Gilat, S. L.; Kawai, S. H.; Lehn, J.-M. *Chem. Eur. J.* **1995**, *53*, 6136.

[16] Kitagawa, D.; Sasaki, K.; Kobatake, S. *Chem. Lett.* **2011**, *84*, 141.

[17] Patel, P. D.; Masunov, A. E. *J. Phys. Chem. C.* **2011**, *115*, 10292.

[18] Matsuda, K. *et. al. J. Phys. Chem. C.* **2008**, *112*, 17005.

[19] Odo, Y.; Matsuda, K.; Irie, M. *Chem. Eur. J.* **2006**, *12*, 4283.

[20] Zhang, J. *et. al. ACS Nano*. **2011**, *5*, 5936.

[21] Förster, T. in *Modern Quantum Chemistry Part III: Action of Light and Organic Crystals*; Sinanoglu, O., Ed.; Academic Press: New York, 1965; pp 93.

[22] Kavarnos, G. J. *Fundamentals of Photoinduced Electron Transfer*; VCH Publishers: New York, 1993.

[23] Sandros, M. G.; Gao, D.; Benson, D. E. *J. Am. Chem. Soc.* **2005**, *127*, 12198.

[24] Zhang, C.-Y.; Yeh, H.-C.; Kuroki, M. T.; Wang, T.-H. *Nature Mater.* **2005**, *4*, 826.

[25] Cseresnyes, Z.; Schwarz, U.; Green, C. M. *BMC Cell Biol.* **2009**, *10:*88.

[26] Jares-Erijman, E.; Giordano, L.; Spagnuolo, C. *Mol. Cryst. Liq. Cryst.* **2005**, *430*, 257.

[27] Berberich, M.; Krause, A.-M.; Orlandi, M.; Scandola, F.; Würthner, F. *Angew. Chem. Int. Ed.* **2008**, *47*, 6616.

[28] Donegá, C. M.; Koole, R. *J. Phys. Chem. C*, **2009**, *113*, 6511.

[29] Raymo, F. M.; Yildiz, I. *Phys. Chem. Chem. Phys.* **2007**, *9*, 2036.

[30] Chan, W. C. W.; Nie, S. *Science*, **1998**, *281*, 2016.

[31] Frasco, M. F.; Chaniotakis, N. *Anal. Bioanal. Chem.* **2010**, *396*, 229.

[32] Gao, X. *et. al. Curr. Opin. Biotechnol.* **2005**, *16*, 63.

[33] Zhu, L.; Zhu, M.-Q.; Hurst, J. K.; Li, A. D. Q. *J. Am. Chem. Soc.* **2005**, *127*, 8968.

[34] Medintz, I. L.; Trammell, S. A.; Mattoussi, H.; Mauro, J. M. *J. Am. Chem. Soc.* **2004**, *126*, 30.

[35] Tomasulo, M.; Yildiz, I.; Raymo, F. M. *Aust. J. Chem.* **2006**, *59*, 175.

[36] Yildiz, I.; Raymo, F. M. *J. Mater. Chem.* **2006**, *16*, 1118.

[37] Skaff, H.; Emerick, T. *Chem. Commun.* **2003**, 52.

[38] Bertelson, R. C. in *Organic Photochromic and Thermochromic Compounds*; Crano, J. C.; Guglielmetti, R. J., Eds.; Plenum: New York 1999; Vol. 1, pp 60.

[39] Erno, Z.; Yildiz, I.; Gorodetsky, B.; Raymo, F. M.; Branda, N. R. *Photochem. Photobiol. Sci.* **2010**, *9*, 249.

[40] Lucas, L. N.; de Jong, J. J. D.; van Esch, J. F.; Kellogg, R. M.; Feringa, B. L. *Eur. J. Org. Chem.* **2003**, 155.

[41] Qin, B.; Yao, R.; Zhiao, X.; Tian, H. *Org. Biomol. Chem.* **2003**, *1*, 2187.

[42] Häupl, T.; Lomoth, R.; Hammarström, L. *J. Phys. Chem. A* **2003**, *107*, 435.

[43] Dale, R. E.; Eisinger, J.; Blumberg, W. E. *Biophys. J.* **1979**, *26*, 161.

[44] Halgren, T. A. *J. Comp. Chem.* **1996**, 490.

[45] Marcus, R. A. *J. Chem. Phys.* **1965**, *43*, 679.

[46] Rehm, D.; Weller, A. *Isr. J. Chem.* **1970**, *8*, 259.

[47] Querner, C.; Reiss, P.; Sadki, S.; Zagorska, M.; Pron, A. *Phys. Chem. Chem. Phys.* **2005**, *7*, 3204.

[48] Ai, X.; Anderson, N. A.; Guo, J. C.; Lian, T. Q. *J. Phys. Chem. B.* **2005**, *109*, 7088.

[49] Kwart, H.; Burchuk, I. *J. Am. Chem. Soc.* **1952**, *74*, 3094.

[50] (a) Sauer, J.; Sustmann, R. *Angew. Chem. Int. Ed. Engl.* **1980**, *19*, 779. (b) Ginsburg, D. *Tetrahedron* **1983**, *39*, 2095.

[51] McElhanon, J. R. *et. al. Langmuir* **2005**, *21*, 3259.

[52] Norris, J. L.; Porter, N. A.; Caprioli, R. M. *Anal. Chem.* **2003**, *75*, 6642.

[53] Emmanuel, E. *et. al. Environ. Int.* **2005**, *31*, 399.

[54] Murphy, M. G. *et. al. Chemosphere* **2005**, *59*, 235.

[55] Metcalfe, T. L.; Dillon, P. J.; Metcalfe, C. D. *Environ. Toxicol. Chem.* **2008**, *27*, 811.

[56] Chen, X. *et. al. Science* **2002**, 295, 1698.

[57] Boul, P. J.; Reutenauer, P.; Lehn, J.-M. *Org. Lett.* **2005**, *7*, 15.

[58] Lehn, J.-M. *Chem. Eur. J.***1999**, *5*, 2455..

[59] Ramström, O.; Lehn, J.-M. *Nat. Rev. Drug Discovery* **2001**, *1*, 26.

[60] Lemieux, V.; Gauthier, S.; Branda, N. R. *Angew. Chem. Int. Ed.* **2006**, *45*, 6820.

[61] (a) Kohler, E. P.; Kable, J. *J. Am. Chem. Soc.* **1935**, *57*, 917. (b) Woodward, R. B.; Baer, H. *J. Am. Chem. Soc.* **1944**, *66*, 645.

[62] (a) Ireland, C. J.; Jones, K.; Pizey, J. S.; Johnson, S. *Synth. Commun.* **1976**, *6*, 185. (b) Hall, H. K., Jr.; Padias, A. B.; Way, T.-F.; Bergmani, B. *J. Org. Chem.* **1987**, *52*, 5528.

[63] (a) Woodward, R. B.; Baer, H. *J. Am. Chem. Soc.* **1948**, *70*, 1161. (b) Anet, F. A. L. *Tetrahedron Lett.* **1962**, *3*, 1219.

[64] Mee, S. P. H.; Lee, V.; Baldwin, J. W.; Crowley, A. *Tetrahedron* **2004**, *60*, 3695.

[65] Fernández-Acebes, A.; Lehn, J.-M. *Adv. Mater.* **1998**, *10*, 1519.

[66] Irie, M.; Lifka, T.; Kobatake, S.; Kato, N. *J. Am. Chem. Soc.* **2000**, *122*, 4871.

[67] Kühni, J.; Adamo, V.; Belser, P. *Synthesis*, **2006**, *12*, 1946.

[68] Oh, C. H.; Lim, Y. M. *Bull. Korean Chem. Soc.*, **2002**, *23*, 663.

[69] (a) Watanabe, M.; Yoshie, N. *Polymer*, **2006**, *47*, 4946. (b) Gandini, A.; Coelho, D.; Silvestre, A. J. D. *Eur. Polym. J.* **2008**, *44*, 4029.

[70] Connors, K. A. *Chemical Kinetics: the Study of Reaction Rates in Solution*, VCH Publishers: New York, 1991.

[71] Myles, A. J.; Zhang, Z.; Liu, G.; Branda, N. R. *Org. Lett.* **2000**, *2*, 2749.

[72] Wigglesworth, T. J.; Branda, N. R. *Adv. Mater.* **2004**, *16*, 123.

[73] McShane, G. J.; Boutchich, M.; Srikantha Phani, A.; Moore, D. F.; Lu, T. J. *J. Micromech. Microeng.* **2006**, *16*, 1926.